INSTITUTE OF PHYSICS PUBLISHING REPORTS ON PROGRESS IN PHYSICS

Rep. Prog. Phys. **66** (2003) 2069–2110 PII: S0034-4885(03)33852-7

Quantum phase transitions

Matthias Vojta

Institut für Theorie der Kondensierten Materie, Universität Karlsruhe,
Postfach 6980, D-76128 Karlsruhe, Germany

E-mail: vojta@tkm.physik.uni-karlsruhe.de

Received 1 August 2003, in final form 8 October 2003
Published 3 November 2003
Online at stacks.iop.org/RoPP/66/2069

Abstract

In recent years, quantum phase transitions have attracted the interest of both theorists and experimentalists in condensed matter physics. These transitions, which are accessed at zero temperature by variation of a non-thermal control parameter, can influence the behaviour of electronic systems over a wide range of the phase diagram. Quantum phase transitions occur as a result of competing ground state phases. The cuprate superconductors which can be tuned from a Mott insulating to a d-wave superconducting phase by carrier doping are a paradigmatic example. This review introduces important concepts of phase transitions and discusses the interplay of quantum and classical fluctuations near criticality. The main part of the article is devoted to bulk quantum phase transitions in condensed matter systems. Several classes of transitions will be briefly reviewed, pointing out, e.g., conceptual differences between ordering transitions in metallic and insulating systems. An interesting separate class of transitions is boundary phase transitions where only degrees of freedom of a subsystem become critical; this will be illustrated in a few examples. The article is aimed at bridging the gap between high-level theoretical presentations and research papers specialized in certain classes of materials. It will give an overview on a variety of different quantum transitions, critically discuss open theoretical questions, and frequently make contact with recent experiments in condensed matter physics.

 © 2003 IOP Publishing Ltd Printed in the UK

Contents

1. Introduction

Phase transitions play an essential role in nature. Everyday examples include the boiling of water or the melting of ice, and more complicated is the transition of a metal into the superconducting state upon lowering the temperature. The universe itself is thought to have passed through several phase transitions as the high-temperature plasma formed by the Big Bang cooled to form the world as we know it today.

Phase transitions occur upon variation of an external control parameter; their common characteristic is a qualitative change in the system properties. The phase transitions mentioned so far occur at a finite temperature; here macroscopic order (e.g. the crystal structure in the case of melting) is destroyed by thermal fluctuations. During recent years, a different class of phase transitions has attracted the attention of physicists, namely transitions taking place at zero temperature. A non-thermal control parameter such as pressure, magnetic field, or chemical composition is varied to access the transition point. There, order is destroyed solely by quantum fluctuations which are rooted in the Heisenberg uncertainty principle.

Quantum phase transitions [1–4] have become a topic of great interest in current condensed matter physics. At first glance it might appear that the study of such special points in the phase diagram is a marginal problem, of interest only to specialists, as such transitions occur at only one special value of a control parameter at the experimentally impossible temperature of absolute zero. However, experimental and theoretical developments in the last decades have clearly established the contrary. They have made clear that the presence of such zero-temperature quantum critical points (QCPs) holds the key to so-far unsolved puzzles in many condensed matter systems. Examples include rare-earth magnetic insulators [5], heavy-fermion compounds [6, 7] high-temperature superconductors [8, 9], and two-dimensional electron gases [1, 10].

As we will see later, quantum critical behaviour, arising from the peculiar excitation spectrum of the quantum critical ground state, can influence measurable quantities over a wide range of the phase diagram. The physical properties of the quantum fluctuations, which can destroy long-range order at absolute zero, are quite distinct from those of the thermal fluctuations responsible for traditional, finite-temperature phase transitions. In particular, the quantum system is described by a complex-valued wavefunction, and the dynamics of its phase near the QCP requires novel theories that have no analogue in the traditional framework of phase transitions.

This article is intended as a primarily non-technical introduction to the field of quantum phase transitions and could serve as a reference for both theorists and experimentalists interested in the field. In section 2, we start with summarizing the basics of finite-temperature phase transitions, extend those general concepts to $T = 0$, highlighting the interplay between classical and quantum fluctuations near a QCP, and illustrate the correspondence between quantum transitions in d and classical transitions in $D = d + z$ dimensions, where z is the dynamic critical exponent. In addition, we briefly discuss some aspects of the theoretical description of phase transitions, such as order parameter field theories and their renormalization group (RG) analysis. Section 3 is devoted to a concrete description of several classes of bulk quantum phase transitions, where 'bulk' refers to the fact that the whole system becomes critical. The discussion includes conventional transitions involving spin or charge order as well as metal–insulator and superconductor–insulator transitions; it is intended to summarize some of the settled and open issues in the field and to make contact with experiments. For more technical details the reader is referred to the references. In section 4 we introduce the so-called boundary quantum phase transitions—these are transitions where only degrees of freedom of a subsystem become critical. This concept is illustrated using examples of quantum impurity

problems, which are of current interest both in correlated bulk materials and in mesoscopic physics. We end in section 5 with a brief summary and outlook. To shorten notations, we will often employ units such that $\hbar = k_B = 1$.

2. Quantum phase transitions

This section will give a general introduction to both classical and quantum phase transitions, and point out similarities and important conceptual differences between the two.

2.1. Basic concepts of phase transitions

We start out with briefly collecting the basic concepts of phase transitions and critical behaviour [11,12] that are necessary for the later discussions. Phase transitions are traditionally classified into first-order and continuous transitions. At first-order transitions the two phases co-exist at the transition temperature—examples are ice and water at 0°C, or water and steam at 100°C. In contrast, at continuous transitions the two phases do not co-exist. An important example is the ferromagnetic transition of iron at 770°C, above which the magnetic moment vanishes. This phase transition occurs at a point where thermal fluctuations destroy the regular ordering of magnetic moments—this happens continuously in the sense that the magnetization vanishes continuously when approaching the transition from below. The transition point of a continuous phase transition is also called the critical point. The study of phase transitions, continuous phase transitions in particular, has been one of the most fertile branches of theoretical physics in the last decades.

In the following, we concentrate on systems near a continuous phase transition. Such a transition can usually be characterized by an order parameter—this is a thermodynamic quantity that is zero in one phase (the disordered) and non-zero and non-unique in the other (the ordered) phase. Very often the choice of an order parameter for a particular transition is obvious as, e.g. for the ferromagnetic transition, where the total magnetization is an order parameter. However, in some cases finding an appropriate order parameter is complicated and still a matter of debate, e.g. for the interaction-driven metal–insulator transition in electronic systems (the Mott transition [13]).

While the thermodynamic average of the order parameter is zero in the disordered phase, its fluctuations are non-zero. If the critical point is approached, the spatial correlations of the order parameter fluctuations become long-ranged. Close to the critical point their typical length scale, the correlation length, ξ, diverges as

$$\xi \propto |t|^{-\nu}, \tag{1}$$

where ν is the correlation length critical exponent and t is some dimensionless measure of the distance from the critical point. If the transition occurs at a non-zero temperature T_c, it can be defined as $t = |T - T_c|/T_c$. In addition to the long-range correlations in space there are analogous long-range correlations of the order parameter fluctuations in time. The typical timescale for a decay of the fluctuations is the correlation (or equilibration) time, τ_c. As the critical point is approached the correlation time diverges as

$$\tau_c \propto \xi^z \propto |t|^{-\nu z}, \tag{2}$$

where z is the dynamic critical exponent. Close to the critical point there is no characteristic length scale other than ξ and no characteristic timescale other than τ_c. (Note that a microscopic cutoff scale must be present to explain non-trivial critical behaviour; for details see, e.g. Goldenfeld [12]. In a solid such a scale is, e.g., the lattice spacing.)

The divergences (1) and (2) are responsible for the so-called critical phenomena. At the phase transition point, correlation length and time are infinite, fluctuations occur on all length scales and timescales, and the system is said to be scale-invariant. As a consequence, all observables depend via power laws on the external parameters. The set of corresponding exponents—called critical exponents—completely characterizes the critical behaviour near a particular phase transition.

Let us illustrate the important concept of scaling in more detail. To be specific, consider a classical ferromagnet with the order parameter being the magnetization, $M(\boldsymbol{r})$. The external parameters are the reduced temperature, $t = |T - T_c|/T_c$, and the external magnetic field, B, conjugate to the order parameter. Close to the critical point the correlation length is the only relevant length scale; therefore the physical properties must be unchanged if we rescale all lengths in the system by a common factor and at the same time adjust the external parameters in such a way that the correlation length retains its old value. This gives rise to the homogeneity relation for the singular part of the free energy density,

$$f(t, B) = b^{-d} f(tb^{1/\nu}, Bb^{y_B}). \tag{3}$$

Here, y_B is another critical exponent. The scale factor, b, is an arbitrary positive number. Analogous homogeneity relations for other thermodynamic quantities can be obtained by differentiating f. The homogeneity law (3) was first obtained phenomenologically by Widom [14]; within the framework of the RG theory [15] it can be derived from first principles.

In addition to the critical exponents ν, y_B, and z defined earlier, a number of other exponents are in common use. They describe the dependence of the order parameter and its correlations with the distance from the critical point and with the field conjugate to the order parameter. The definitions of the most commonly used critical exponents are summarized in table 1. Note that not all the exponents defined in table 1 are independent of each other. The four thermodynamic exponents, α, β, γ, and δ, can all be obtained from the free energy (3), which contains only two independent exponents. They are therefore connected by the so-called scaling relations

$$2 - \alpha = 2\beta + \gamma, \qquad 2 - \alpha = \beta(\delta + 1). \tag{4}$$

Analogously, the exponents of the correlation length and correlation function are connected by two so-called hyperscaling relations

$$2 - \alpha = d\nu, \qquad \gamma = (2 - \eta)\nu. \tag{5}$$

(Hyperscaling relations are violated in theories with mean-field critical behaviour due to the presence of a dangerously irrelevant variable, see section 2.6.) Since statics and dynamics decouple in classical statistics (section 2.3) the dynamic exponent z is completely independent of all the others.

Table 1. Commonly used critical exponents for magnets, where the order parameter is the magnetization, m, and the conjugate field is a magnetic field, B. t denotes the distance from the critical point and d is the space dimensionality. (The exponent y_B defined in (3) is related to δ by $y_B = d\delta/(1 + \delta)$.)

	Exponent	Definition	Conditions
Specific heat	α	$C \propto \lvert t\rvert^{-\alpha}$	$t \to 0$, $B = 0$
Order parameter	β	$m \propto (-t)^{\beta}$	$t \to 0$ from below, $B = 0$
Susceptibility	γ	$\chi \propto \lvert t\rvert^{-\gamma}$	$t \to 0$, $B = 0$
Critical isotherm	δ	$B \propto \lvert m\rvert^{\delta}\mathrm{sign}(m)$	$B \to 0$, $t = 0$
Correlation length	ν	$\xi \propto \lvert t\rvert^{-\nu}$	$t \to 0$, $B = 0$
Correlation function	η	$G(r) \propto \lvert r\rvert^{-d+2-\eta}$	$t = 0$, $B = 0$
Dynamic	z	$\tau_c \propto \xi^z$	$t \to 0$, $B = 0$

One of the most remarkable features of continuous phase transitions is universality, i.e. the fact that the critical exponents are the same for entire classes of phase transitions that may occur in very different physical systems. These universality classes are determined only by the symmetries of the order parameter and by the space dimensionality of the system. This implies that the critical exponents of a phase transition occurring in nature can be determined exactly (at least in principle) by investigating any simple model system belonging to the same universality class. The mechanism behind universality is again the divergence of the correlation length. Close to the critical point the system effectively averages over large volumes, rendering the microscopic details of the Hamiltonian unimportant.

2.2. Quantum mechanics and the vicinity of the critical point

The question of to what extent quantum mechanics is important for understanding a continuous phase transition has at least two aspects. On the one hand, quantum mechanics can be essential to understand the existence of the ordered phase (e.g. superconductivity)—this depends on the particular transition considered. On the other hand, one may ask whether quantum mechanics influences the asymptotic critical behaviour. For this discussion we have to compare two energy scales, namely $\hbar\omega_c$, which is the typical energy of long-distance order parameter fluctuations, and the thermal energy, $k_B T$. We have seen in the preceding section that the typical timescale, τ_c, of the fluctuations diverges as a continuous transition is approached. Correspondingly, the typical frequency scale, ω_c, goes to zero and with it the typical energy scale

$$\hbar\omega_c \propto |t|^{\nu z}. \tag{6}$$

Quantum mechanics will be important as long as this typical energy scale is larger than the thermal energy, $k_B T$; on the other hand, for $\hbar\omega_c \ll k_B T$ a purely classical description can be applied to the order parameter fluctuations. In other words, the character of the order parameter fluctuations crosses over from quantum to classical when $\hbar\omega_c$ falls below $k_B T$.

Now, for any transition occurring at some finite temperature T_c, quantum mechanics will become unimportant for $|t| < T_c^{1/\nu z}$; in other words, the critical behaviour asymptotically close to the transition is entirely classical. This justifies calling all finite-temperature phase transitions 'classical'. Quantum mechanics can still be important on microscopic scales, but classical thermal fluctuations dominate on the macroscopic scales that control the critical behaviour. If, however, the transition occurs at zero temperature as a function of a non-thermal parameter, r, like pressure or magnetic field, the behaviour is always dominated by quantum fluctuations. Consequently, transitions at zero temperature are called 'quantum' phase transitions.

The interplay of classical and quantum fluctuations leads to an interesting phase diagram in the vicinity of the QCP. Two cases need to be distinguished, depending on whether long-range order can exist at finite temperatures.

Figure 1(a) describes the situation where order only exists at $T = 0$; this is the case, e.g., in two-dimensional magnets with SU(2) symmetry where order at finite T is forbidden by the Mermin–Wagner theorem. In this case there will be no true phase transition in any real experiment carried out at finite temperature. However, the finite-T behaviour is characterized by three very different regimes, separated by crossovers, depending on whether the behaviour is dominated by thermal or quantum fluctuations of the order parameter. In the thermally disordered region the long-range order is destroyed mainly by thermal order parameter fluctuations. In contrast, in the quantum disordered region the physics is dominated by quantum fluctuations, the system essentially resembles that in its quantum disordered ground state at $r > r_c$. In between is the so-called quantum critical region [16], where both types of

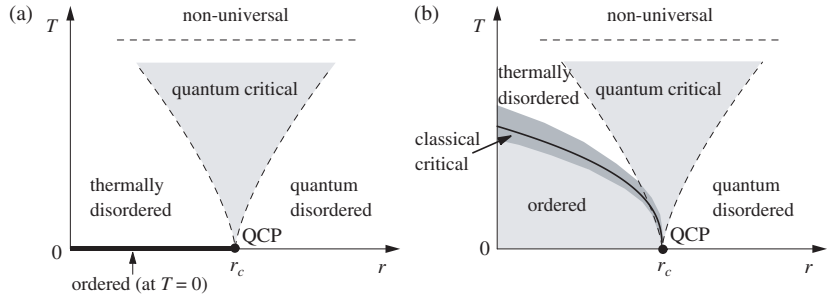

Figure 1. Schematic phase diagrams in the vicinity of a QCP. The horizontal axis represents the control parameter r used to tune the system through the quantum phase transition, and the vertical axis is the temperature, T. (*a*) Order is only present at zero temperature. The dashed lines indicate the boundaries of the quantum critical region where the leading critical singularities can be observed; these crossover lines are given by $k_B T \propto |r - r_c|^{\nu z}$. (*b*) Order can also exist at finite temperature. The solid line marks the finite-temperature boundary between the ordered and disordered phases. Close to this line, the critical behaviour is classical.

fluctuations are important. It is located near the critical parameter value $r = r_c$ at comparatively high (!) temperatures. Its boundaries are determined by the condition $k_B T > \hbar\omega_c \propto |r - r_c|^{\nu z}$: the system 'looks critical' with respect to the tuning parameter r, but is driven away from criticality by thermal fluctuations. Thus, the physics in the quantum critical region is controlled by the thermal excitations of the quantum critical ground state, whose main characteristic is the absence of conventional quasiparticle-like excitations. This causes unusual finite-temperature properties in the quantum critical region, such as unconventional power laws, non-Fermi liquid behaviour, etc. Universal behaviour is only observable in the vicinity of the QCP, i.e. when the correlation length is much larger than microscopic length scales. Quantum critical behaviour is thus cut off at high temperatures when $k_B T$ exceeds characteristic microscopic energy scales of the problem—in magnets this cutoff is, e.g., set by the typical exchange energy.

If order also exists at finite temperatures (figure 1(*b*)) the phase diagram is even richer. Here, a real phase transition is encountered upon variation of r at low T; the QCP can be viewed as the endpoint of a line of finite-temperature transitions. As discussed earlier, classical fluctuations will dominate in the vicinity of the finite-T phase boundary, but this region becomes narrower with decreasing temperature, such that it might even be unobservable in a low-T experiment. The fascinating quantum critical region is again at finite temperatures above the QCP.

A QCP can be generically approached in two different ways: $r \to r_c$ at $T = 0$ or $T \to 0$ at $r = r_c$. The power-law behaviour of physical observables in both cases can often be related. Let us discuss this idea by looking at the entropy, S. It goes to zero at the QCP (exceptions are impurity transitions discussed in section 4), but its derivatives are singular. The specific heat $C = T\partial S/\partial T$ is expected to show power-law behaviour, as does the quantity $B = \partial S/\partial r$. Using scaling arguments (see later), one can now analyse the ratio of the singular parts of B and C: the scaling dimensions of T and S cancel, and therefore B/C scales as the inverse of the tuning parameter r. Thus, one obtains a universal divergence in the low-temperature limit, $B/C \propto |r - r_c|^{-1}$; similarly, $B/C \propto T^{-1/\nu z}$ at $r = r_c$ [17]. Note that B/C does not diverge at a finite-temperature phase transition. At a pressure-tuned phase transition $r \equiv p$, B measures the thermal expansion, and B/C is the so-called Grüneisen parameter. As will be discussed in section 2.6, the scaling argument presented here can be invalid above the upper-critical dimension.

2.3. Quantum–classical mapping and scaling

To gain a deeper understanding of the relation between classical and quantum behaviour, and the possible quantum–classical crossover, we have to recall general features from quantum statistical mechanics.

The starting point for the derivation of thermodynamic properties is the partition function

$$Z = \mathrm{Tr}\, \mathrm{e}^{-H/k_\mathrm{B}T}, \tag{7}$$

where $H = H_\mathrm{kin} + H_\mathrm{pot}$ is the Hamiltonian characterizing the system. In a classical system, the kinetic and potential part of H commute; thus Z factorizes, $Z = Z_\mathrm{kin} Z_\mathrm{pot}$, indicating that in a classical system statics and dynamics decouple. The kinetic contribution to the free energy will usually not display any singularities since it derives from the product of simple Gaussian integrals. Therefore, one can study classical phase transitions using effective time-independent theories, which naturally live in d dimensions.

In contrast, in a quantum problem the kinetic and potential parts of H in general do not commute, and the quantum mechanical partition function does not factorize, which implies that statics and dynamics are always coupled. An order parameter field theory needs to be formulated in terms of space- and time-dependent fields. The canonical density operator $\mathrm{e}^{-H/k_\mathrm{B}T}$ looks exactly like a time evolution operator in imaginary time τ if one identifies $1/k_\mathrm{B}T = \tau = -\mathrm{i}\Theta/\hbar$, where Θ denotes the real time. Therefore, it proves convenient to introduce an imaginary time direction into the system—formally this is done in the path integral representation of the partition function. At zero temperature the imaginary time acts similar to an additional space dimension since the extension of the system in this direction is infinite. According to (2), time scales like the zth power of a length. (Note that $z = 1$ for many transitions in clean insulators; however, in general other values of z including fractional ones can occur.) The classical homogeneity law (3) for the free energy density can now easily be adopted to the case of a quantum phase transition. At zero temperature it reads

$$f(t, B) = b^{-(d+z)} f(tb^{1/\nu}, Bb^{y_\mathrm{B}}), \tag{8}$$

where now $t = |r - r_\mathrm{c}|/r_\mathrm{c}$. This shows that a quantum phase transition in d space dimensions is related to a classical transition in $(d + z)$ space dimensions.

For a quantum system, it is now interesting to discuss the quantum-to-classical crossover upon approaching a finite-temperature phase transition—this turns out to be equivalent to a dimensional crossover. Under the quantum–classical mapping the temperature of the quantum problem maps onto the inverse length of the imaginary time axis. (Note that the temperature of the classical problem corresponds to a coupling constant in the quantum model within this mapping.) Close to the transition (figure 1(b)) the behaviour is determined by the relation between the characteristic correlation time, τ_c, and the extension in imaginary time direction, $\beta = 1/k_\mathrm{B}T$. The crossover from quantum to classical behaviour will occur when the correlation time, τ_c, becomes larger than β, which is equivalent to the condition $|t|^{\nu z} < k_\mathrm{B}T$; in other words, once $\tau_\mathrm{c} > \beta$, the system realizes that it is effectively only d-dimensional and not $(d + z)$-dimensional. The corresponding crossover scaling is equivalent to finite size scaling in imaginary time direction.

In contrast, when approaching a zero-temperature transition by lowering the temperature at $r = r_\mathrm{c}$, both $1/k_\mathrm{B}T$ and τ_c diverge, such that quantum effects are always important, and we get a truly $(d + z)$-dimensional system. Recognizing that quantum critical singularities can be cut off both by tuning r away from r_c at $T = 0$ and by raising T at $r = r_\mathrm{c}$, it is useful to generalize the homogeneity law (8) to finite temperatures,

$$f(t, B, T) = b^{-(d+z)} f(tb^{1/\nu}, Bb^{y_\mathrm{B}}, Tb^{z}). \tag{9}$$

The homogeneity law for the free energy immediately leads to scaling behaviour of both static and dynamic observables. Consider an observable $\mathcal{O}(k, \omega)$, e.g. a magnetic susceptibility, measured at wavevector, k, and frequency, ω; the existence of a single length scale, ξ, and a single timescale, $\omega_c^{-1} = \xi^z$, implies

$$\begin{aligned}\mathcal{O}(t, k, \omega, T) &= \xi^{d_\mathcal{O}} O_1(k\xi, \omega\xi^z, T\xi^z) \\ &= T^{-d_\mathcal{O}/z} O_2\left(kT^{-1/z}, \frac{\omega}{T}, T\xi^z\right),\end{aligned} \tag{10}$$

where O_1 and O_2 are different forms for the scaling function associated with the observable $\mathcal{O}$, and $d_\mathcal{O}$ is the so-called scaling dimension of $\mathcal{O}$. For simplicity, we have set the external field $B = 0$ and assumed that k is measured relative to the ordering wavevector.

Precisely at the critical point, where the correlation length is infinite, the only length is set by the measurement wavevector k; analogously, the only energy is ω, leading to

$$\mathcal{O}(t = 0, k, \omega, T = 0) = k^{-d_\mathcal{O}} O_3\left(\frac{k^z}{\omega}\right). \tag{11}$$

Similarly, for $k = 0$, but finite temperatures, we obtain

$$\mathcal{O}(t = 0, k = 0, \omega, T) = T^{-d_\mathcal{O}/z} O_4\left(\frac{\omega}{T}\right); \tag{12}$$

this is known as 'ω/T' scaling. It is important to note that the relations (10)–(12), sometimes also called 'naive scaling', are only expected to be valid if the critical point satisfies hyperscaling properties, which is true below the upper-critical dimension (see section 2.6).

The power of the quantum–classical analogy can be nicely demonstrated by considering a correlation function at the critical point. In a classical d-dimensional system, correlations typically fall off with a power law in real space, implying a momentum space behaviour as

$$G(k) \propto k^{-2+\eta_d}. \tag{13}$$

If we are now interested in a quantum phase transition with $z = 1$ which maps onto a $(d + 1)$-dimensional classical theory with known properties, we can conclude that at $T = 0$

$$G(k, \mathrm{i}\omega_n) \propto [k^2 + \omega_n^2]^{(-2+\eta_{d+1})/2} \tag{14}$$

where the Matsubara frequency ω_n simply takes the role of an additional wavevector component. For real frequencies, the above translates into a retarded Green's function of the form

$$G^R(k, \omega) \propto [k^2 - (\omega + \mathrm{i}\delta)^2]^{(-2+\eta_{d+1})/2}. \tag{15}$$

This examples illustrates the character of the excitation spectrum at a QCP: G^R does not show a conventional quasiparticle pole, but instead a branch cut for $\omega > k$, corresponding to a critical continuum of excitations. This implies that modes become overdamped, and the system shows quantum relaxational dynamics [3].

Now, if a quantum transition seems to map generically onto a classical transition, what is different about quantum transitions? For a number of reasons it turns out that not all required properties of a given quantum system can be obtained from a classical theory, the reasons being:

(A) Theories for quantum systems can have ingredients that make them qualitatively different from their classical counterparts; examples are topological Berry phase terms and long-ranged effective interactions arising from soft modes.
(B) Even if a quantum–classical mapping is possible, calculating real time dynamics of the quantum system often requires careful considerations and novel theories, as an approximation done on the imaginary time axis is in general not appropriate for real times [3].

(C) Quenched disorder leads to an extreme anisotropy in space–time in the classical theory [18] (see section 3.3).

(D) The dynamic properties of the quantum system near a QCP are characterized by a fundamental new timescale, the phase coherence time, τ_ϕ, which has no analogue at the corresponding classical transition [3]. Notably, τ_ϕ diverges as $T \to 0$ for all parameter values, i.e. the quantum system has perfect phase coherence even in the disordered phase—this seems to be peculiar, considering that all correlations decay exponentially in the high-temperature phase of the corresponding $(d+z)$-dimensional classical model. Technically, this peculiarity is related to the nature of the analytic continuation between imaginary and real times. In many models for quantum phase transitions, it is found that $\tau_\phi \propto 1/T$ as $T \to 0$ at the critical coupling, but τ_ϕ diverges faster in the stable phases.

Parenthetically, we note that 'conventional' quantum criticality leads to a power law behaviour in dynamic observables as a function of energy and momentum, where (at $T = 0$) the singularity is cut off both by finite frequency and finite momentum (measured from the ordering wavevector). There are, however, interesting cases where the order parameter is not associated with a particular momentum, and then so-called 'local' critical behaviour may occur. Candidate transitions are those involving spin glass or topological order; interesting recent proposals involve the breakdown of Kondo screening in heavy-fermion compounds (section 3.2.3).

2.4. Ground state properties near a quantum phase transition

It is useful to think about a quantum transition from the point of view of many-body eigenstates of the system. A quantum phase transition is a non-analyticity of the ground state properties of the system as a function of the control parameter r. If this singularity arises from a simple level crossing in the many-body ground state, then we have a first-order quantum phase transition, without diverging correlations and associated critical singularities. A first-order quantum transition can also occur in a finite-size system. The situation is different for continuous transitions, where a higher-order singularity in the ground state energy occurs: here an infinite number of many-body eigenstates are involved, and the thermodynamic limit is required to obtain a sharp transition. For any finite-size system a continuous transition will be rounded into a crossover—this is nothing but an avoided level crossing in the ground state, which then becomes infinitely sharp in the thermodynamic limit.

For numerical simulations of finite-size systems the choice of boundary conditions plays an important role: if the infinite system shows a first-order transition where the two ground states can be distinguished by a certain quantum number, then such a transition will also be rounded into a crossover for finite system size if the boundary conditions spoil the existence of this quantum number. This applies, e.g., to simulations using open boundary conditions that invalidate momentum or a certain parity as good quantum numbers.

2.5. Order parameters and order parameter field theories

Near a phase transition the relevant physics is described by long-wavelength order parameter fluctuations. Therefore, it appears appropriate to disregard microscopic processes and to work with a theory containing the order parameter fluctuations only. However, in itinerant electron systems it can be neccessary to include low-energy fermionic excitations explicitly in the critical theory [19] because of the strong coupling between order parameter and fermionic particle–hole modes (see sections 3.2.3 and 3.2.4).

Formally, an effective theory can be obtained in the path integral formulation from a microscopic model of interacting particles (e.g. fermions). To this end, the interaction terms are suitably decoupled via a Hubbard–Stratonovich transformation, and then the microscopic degrees of freedom can be integrated out, resulting in a theory of the order parameter fluctuations alone. Near a phase transition, the correlation length is large, and therefore the effective theory can be formulated in the continuum limit, with a proper ultraviolet cutoff set by the lattice spacing. In most cases the resulting theory will contain simple powers of the order parameter field and its gradients, and the form of such a theory can actually be derived based on symmetry arguments only. The form of the low-energy effective action will thus depend only on the dimensionality and symmetry of the underlying system and the symmetry of the order parameter—reflecting nothing but the celebrated universality of critical behaviour.

In the following we mention a few examples of models and corresponding quantum field theories; concrete applications will be given in section 3. We will not discuss here the special theories appropriate for one-dimensional systems, and the reader is referred to [3] for an introduction.

2.5.1. Ising and rotor models. Quantum rotor models, with the Hamiltonian

$$H_{\mathrm{R}} = \frac{Jg}{2} \sum_i \hat{\boldsymbol{L}}_i^2 - J \sum_{\langle ij \rangle} \hat{\boldsymbol{n}}_i \cdot \hat{\boldsymbol{n}}_j \tag{16}$$

are some of the simplest models showing quantum phase transitions. Here, the N-component operators $\hat{\boldsymbol{n}}_i$ with $N \geqslant 2$ represent the orientation of rotors on sites i of a regular d-dimensional lattice, with $\hat{\boldsymbol{n}}_i^2 = 1$, and the $\hat{\boldsymbol{L}}_i$ are the corresponding angular momenta. The nearest-neighbour coupling in the second term prefers a ferromagnetic ordering, whereas the kinetic term tends to delocalize the individual rotors. Thus, $g \ll 1$ leads to an ordered state, whereas $g \gg 1$ places the system into a quantum-disordered phase [3]. A related model with $N = 1$ components is the quantum Ising model discussed in more detail in section 2.8.

The order parameter describing the transition in the model (16) is the ferromagnetic magnetization; a continuum theory can be derived from the lattice model in the path integral formulation by spatial coarse-graining; i.e. the variables $\hat{\boldsymbol{n}}_i$ are averaged over microscopic length scales. The magnitude of the continuum order parameter field, $\boldsymbol{\phi}$, can thus vary over a wide range, although the 'magnitude' of the underlying microscopic object (a single rotor) is fixed. Expanding the resulting action into lowest order field gradients, one arrives at the so-called ϕ^4 theory. This quantum field theory, described by the action

$$\begin{aligned} Z &= \int \mathcal{D}\phi_\alpha(x,\tau) \exp(-\mathcal{S}), \\ \mathcal{S} &= \int d^d x \int_0^{\hbar/k_{\mathrm{B}}T} \mathrm{d}\tau \left[\frac{1}{2}(\partial_\tau \phi_\alpha)^2 + \frac{c^2}{2}(\nabla_x \phi_\alpha)^2 + \frac{r}{2}\phi_\alpha^2 + \frac{g_0}{4!}(\phi_\alpha^2)^2 \right], \end{aligned} \tag{17}$$

turns out to be a generic theory, to which we will refer frequently in this article, being appropriate for systems where the N-component order parameter field, $\phi_\alpha(x,\tau)$, is a non-conserved density. r is the bare 'mass' of the order parameter fluctuations, used to tune the system across the quantum phase transition, and c is the velocity. g_0 describes the important self-interactions of the ϕ fluctuations, and we will comment on them in the next section. Note that the dynamic exponent is $z = 1$, i.e. space and time enter symmetrically. Although the order parameter fluctuations are bosonic in nature, the second-order time derivative in (17) does not represent the dynamics of a canonical boson, but rather arises from a gradient expansion of the order parameter action.

The model equation (17) obeys an O(N) symmetry, corresponding to rotations in order parameter space. $N = 1$ corresponds to a scalar or Ising order parameter; for $N \geqslant 2$ the order parameter represents a vector for which one can distinguish longitudinal (amplitude) and transverse (phase or direction) fluctuations. For $N = 3$, the theory can describe spin degrees of freedom in an insulator; in a number of cases, however, Berry phases are important, which we will explicitly discuss later. In writing down (17), we have assumed ϕ to be real. Situations with complex ϕ can appear as well; then the action can contain two non-linear terms, $(|\phi_\alpha|^2)^2$ and $|\phi_\alpha^2|^2$. We will see in section 3.2.1 that the phase of a complex order parameter field usually corresponds to a sliding degree of freedom of a density wave.

At positive values of r, the model (17) is in a disordered phase, characterized by $\langle\phi\rangle = 0$; at $T = 0$ the propagator of the ϕ fluctuations has a gap of size $\Delta(T = 0) = r$ (to zeroth order in g_0). With decreasing r, this gap decreases, vanishing at the quantum phase transition to the ordered phase. In the ordered phase, the magnitude of the order parameter is determined by g_0; at $T = 0$ at the mean-field level it is $\langle\phi\rangle = -r/(2g_0)$. For $N \geqslant 2$ the ordered phase breaks a continuous symmetry and supports gapless Goldstone modes with linear dispersion.

Near the critical point, for $N \geqslant 2$ both amplitude and phase fluctuations can be important. However, as will be discussed in sections 2.6 and 2.7, below the so-called upper-critical dimension the critical behaviour is determined by phase fluctuations, and in this case a theory that neglects amplitude fluctuation—a 'hard-spin' theory in contrast to the 'soft-spin' formulation of the ϕ^4 model—is adequate. The hard-spin theory is formulated in terms of a field, $n(x, \tau)$, with a unit-length constraint and is known as the non-linear sigma model:

$$Z = \int \mathcal{D}\boldsymbol{n}(x,\tau)\delta(\boldsymbol{n}^2 - 1)\exp(-\mathcal{S}),$$
$$\mathcal{S} = \frac{N}{2cg_0}\int d^d x \int_0^{\hbar/k_B T} \mathrm{d}\tau[(\partial_\tau n_\alpha)^2 + c^2(\nabla_x n_\alpha)^2]. \tag{18}$$

For dimensions $1 < d < 3$, equivalently $2 < \mathcal{D} < 4$ with $\mathcal{D} = d + z$, the ϕ^4 model (17) and the non-linear sigma model (18) represent different approaches to describe the same QCP, and their critical properties are identical [20]. Technically, the ϕ^4 model can be analysed in an expansion about the upper-critical dimension, i.e. for $\mathcal{D} = 4 - \epsilon$, whereas the non-linear sigma model allows an expansion about the lower-critical dimension, $\mathcal{D} = 2 + \epsilon$—those will be briefly discussed in section 2.7.

Both models (17) and (18) possess propagating modes that are undamped at low energies, and the quantum transition is characterized by $z = 1$. In systems with gapless fermionic excitations, order parameter fluctuations can, however, decay into particle–hole pairs, and this damping requires modifications of the described theories (or even different approaches) (see section 3.1).

As usual, theories of the type (17), supplemented by higher order terms and/or suitable coupling to external fields, can also describe first-order transitions. There, the transition point is characterized by the existence of two distinct degenerate global minima in the free-energy landscape, which usually leads to a jump in the order parameter and other observables when tuning the system through the transition. However, no universality is present at first-order transitions, and a continuum description is only appropriate for transitions being weakly first order.

2.5.2. Heisenberg spins. Deriving a continuum model for a system of localized quantum-mechanical spins can be conveniently done using spin-coherent state path integrals, and the reader is referred to [3] for an introduction. The orientation of each spin is described by a three-component unit vector, $\boldsymbol{N}$, and coherent states, $|\boldsymbol{N}\rangle$, obey $\langle\boldsymbol{N}|\hat{S}|\boldsymbol{N}\rangle = S\boldsymbol{N}$. The dynamics

of a single spin takes the form of a Berry phase term, $\mathcal{S}_{\rm B} = \int {\rm d}\tau \langle \boldsymbol{N}|\partial_\tau|\boldsymbol{N}\rangle$, which is purely imaginary. This term can be shown to be equal to iS times the solid angle subtended by the spin vector on the unit sphere (note $\boldsymbol{N}(\beta) = \boldsymbol{N}(0)$)—importantly this Berry phase term contains a first-order time derivative.

The order parameter of interest is again a magnetization density, e.g. for antiferromagnets a staggered magnetization. Starting from a lattice spin model, a continuum action can be derived that contains gradients of the order parameter field, e.g. of the form (17) or (18), plus a term arising from the spin Berry phases [3]. The behaviour of the resulting low-energy theory crucially depends on those Berry phases and is completely different for ferromagnets and antiferromagnets: in ferromagnetic spin systems the Berry phase terms add up and determine the dynamics of the system, as they dominate over the second-order time derivative in (17) or (18)—this is related to the fact that the order parameter is a conserved density here. In contrast, in antiferromagnets the Berry phase contributions oscillate in sign from site to site, and on average simply cancel. Therefore, in many cases Berry phases can essentially be neglected, e.g. in clean antiferromagnets on high-dimensional regular lattices, and the resulting model is a ϕ^4 or non-linear sigma model. However, singular Berry phase configurations can play a role. This is crucial in one space dimension, where a corresponding topological term appears in the action for half-integer spins, which leads to the well-known gapless 'critical' phase with power law decay of spin correlations for the $d = 1$ Heisenberg model. In contrast, for integer spins the topological term is absent, and the system is characterized by an excitation gap and conventional short-range spin correlations.

In a number of cases the analysis of the spin model can be carried out in terms of auxiliary particles. One example is the Dyson–Maleev representation of spin operators in terms of bosons; another one is the bond–boson representation for spin pairs (dimers) in quantum paramagnets [3]. In both situations one arrives at theories similar to Bose gases, which will be discussed below.

2.5.3. Boson and fermion models. Microscopic models of bosons and fermions can have a plethora of ordered phases. In many cases, the order parameter can be represented as a boson or fermion bilinear, as for spin density waves (SDWs) or charge density waves (CDWs), and the critical theory is of ϕ^4-type with proper modifications (section 3.2.3).

In addition, models of bosons or fermions with a conserved charge, Q, can have a transition between a phase where $\langle Q\rangle$ is pinned to a quantized value and a phase where Q varies smoothly as function of external parameters. In those cases, the density is an appropriate order parameter; however, the theory has to be formulated in terms of Bose or Fermi fields and will contain imaginary Berry phase terms for the particle dynamics. For instance, varying the chemical potential through zero drives a quantum phase transition where the zero-temperature particle density is zero in one phase and finite in the other. For bosons in $d > 2$, this dilute gas QCP is the endpoint of a line of finite-T transitions, associated with Bose–Einstein condensation [3].

Interesting physics obtains in the presence of strong local interactions, the Hubbard model being a paradigmatic example. The physics of the fermionic Hubbard model is a subject of vast active research, and cannot be reviewed here (see section 3.4 for some remarks on the Mott–Hubbard metal–insulator transition). The bosonic Hubbard model is somewhat simpler; it was originally introduced to describe spinless bosons on a lattice, representing Cooper pairs undergoing Josephson tunnelling between superconducting islands, with a strong on-site Coulomb repulsion. This model shows superfluid and insulating phases, and an appropriate order parameter is the expectation value of a bosonic field, representing the superfluid density (see section 3.5).

Microscopic realizations of hard-core boson models also arise from models of quantum spins, where the degrees of freedom of spins or spin clusters can be rewritten in terms of bosons with infinite on-site repulsion. A nice example of a dilute Bose gas critical point described earlier is found in quantum antiferromagnets in an external field, where the zero-field ground state is a gapped singlet state: an increasing field splits the triplet excitation energies, and at a critical field, H_c, the lowest triplet condenses, leading to a state with transverse long-range order. Both the $T = 0$ transition and the finite-T transition (present in $d > 2$), where the transverse order is established, can be understood as 'Bose–Einstein condensation of magnons'. Interestingly, the amplitude and phase of the condensate wavefunction correspond to the magnitude and direction of the transverse magnetization, and can thus be measured directly.

2.6. Fluctuations and critical dimensions

The critical behaviour at a particular transition is crucially determined by the role played by fluctuations around the mean-field solution, and their mutual interactions, e.g. the $g_0\phi^4$ term in the ϕ^4 theory. It turns out that fluctuations become increasingly important if the space dimensionality of the system is reduced. Above a certain dimension, called the upper-critical dimension, d_c^+, fluctuations are irrelevant, and the critical behaviour is identical to that predicted by mean-field theory (Ginzburg criterion). For classical systems with short-range interactions and a scalar or vector order parameter one finds $d_c^+ = 4$; the mean-field exponents of the corresponding ϕ^4 theory are:

$$\alpha = 0, \qquad \beta = \tfrac{1}{2}, \qquad \gamma = 1, \qquad \delta = 3, \qquad \nu = \tfrac{1}{2}, \qquad \eta = 0. \tag{19}$$

Between d_c^+ and a second, smaller special dimension, called the lower-critical dimension d_c^-, a phase transition exists, but the critical behaviour is different from mean-field theory. Below d_c^-, fluctuations become so strong that they completely suppress the ordered phase; we have $d_c^- = 2$ for the classical ϕ^4 model with $N > 1$ components.

The quantum–classical mapping discussed earlier implies that for a quantum phase transition the critical dimensions are reduced by z compared with the corresponding classical transition. Thus, in $d = 3$ many quantum transitions show mean-field behaviour (supplemented by logarithmic corrections if $z = 1$).

Technically, the existence of the upper-critical dimension is connected with the role played by the ultraviolet cutoff of the quantum field theory. For $d < d_c^+$ the integrals arising in perturbation theory are ultraviolet convergent, implying that the cutoff can be sent to infinity. Thus, the critical behaviour becomes cutoff-independent, i.e. truly universal, and observables will follow 'naive' scaling, including 'ω/T' scaling in dynamical quantities, as exploited in section 2.3, and exponents will fulfil hyperscaling relations (5). Physically, this universality arises from the fact that the non-linear interaction terms, e.g. g in the ϕ^4 theory, flow towards universal values in the low-energy limit. In contrast, for $d > d_c^+$, quantities will depend on the ultraviolet cutoff, and non-universal corrections to observables arise from the non-linearities of the original theory—these are termed dangerously irrelevant. Critical exponents will be independent of d, and thus hyperscaling is violated.

Importantly, at the critical point in $d < d_c^+$ the integrals arising in perturbation theory are infrared divergent. In other words, (bare) perturbation theory itself is divergent below d_c^+ at $T = 0$. The trick to overcome this problem is the ϵ expansion described in the next section.

For transitions that cannot be easily described by a local order parameter field theory, the situation is less clear. For instance, for the disorder-driven metal–insulator transition (section 3.4) the lower-critical dimension is $d_c^- = 2$; it is likely that an upper-critical dimension does not exist [21].

2.7. RG approach and calculation of observables

A powerful tool for the analysis of order-parameter field theories is the RG approach [15], which is designed to determine the asymptotic low-energy, long-wavelength behaviour of a system. The momentum-shell formulation of the RG proceeds by successively eliminating high-energy degrees of freedom, and at the same time renormalizing the couplings of the theory to keep physical properties invariant. Doing so, the coupling constants flow as a function of the cutoff energy, which is described by differential RG equations. In the low-energy limit, the RG flow reaches a fixed point, and the corresponding fixed point values of the couplings can be trivial (zero or infinity) or non-trivial. The trivial values describe stable phases of the system, whereas non-trivial finite values correspond to so-called intermediate-coupling fixed points, which usually are critical fixed points describing continuous phase transitions.

Analytical RG computations require a perturbative treatment of the interaction terms of the field theory. For $d < d_c^+$ these grow under RG transformations, i.e. interactions are relevant in the RG sense below d_c^+. For the ϕ^4 theory (17) the critical fixed point with non-linearity $g = 0$ (the so-called Gaussian fixed point) is unstable w.r.t. finite g; i.e. the critical fixed point for $d < d_c^+$ will be characterized by a finite value of g (Wilson–Fisher fixed point). The relevance of the interaction implies that bare perturbation theory is divergent at criticality. This problem can be overcome using the so-called ϵ expansion: A theory of the ϕ^4-type can be analysed in an expansion around the upper-critical dimension, i.e. in $\epsilon = d_c^+ - d$. This approach is based on the observation that the fixed point value of renormalized coupling, g, is small near $d = d_c^+$, and a double expansion in g and ϵ allows for controlled calculations. The RG differential equations are used to determine RG fixed points and the corresponding values of the couplings. For example, in the ϕ^4 theory at criticality, the RG equation, describing the flow of the dimensionless non-linear coupling, g, upon reducing the cutoff, Λ, reads

$$\frac{\mathrm{d}g}{\mathrm{d}\ln\Lambda} \equiv \beta(g) = -\epsilon g + \frac{N+8}{6} g^2 + \mathcal{O}(g^3), \tag{20}$$

with a fixed point at $g^* = (6\epsilon)/(N+8)$, where $\epsilon = d_c^+ - d$. Physicswise, the finite value of g at criticality implies strong self-interactions of the order parameter bosons for $d < d_c^+$; furthermore, amplitude fluctuations of the order parameter in a $N \geqslant 2$ ϕ^4 theory are frozen out, and the critical dynamics is carried by phase fluctuations. A different expansion can be applied to the non-linear sigma model (18), namely an expansion around the lower-critical dimension, d_c^-, i.e. the expansion parameter is $\epsilon = d - d_c^-$. Here, the underlying idea is that the transition temperature t is small near $d = d_c^-$, and the double expansion is done in t and ϵ around the ordered state. We note that ϵ expansions are strictly asymptotic expansions, i.e. the limit $\epsilon \to 0$ has to be taken first, and convergence is not guaranteed for any finite ϵ.

Observables at and near criticality require different treatments, depending on whether $d > d_c^+$ or $d < d_c^+$. Above the upper-critical dimension, bare perturbation is usually sufficient. Below d_c^+, one can employ a renormalized perturbation expansion: perturbation theory is formulated in terms of renormalized quantities, and in the final expressions the couplings are replaced by their fixed point values, and the results are interpreted as arising from an ϵ expansion of the expected power-law behaviour; i.e. power laws are obtained by re-exponentiating the perturbation series. The renormalized perturbation expansion can thus be understood as a certain resummation technique of bare perturbation theory. In some cases, a $1/N$ expansion, where N is the number of order parameter components, can also be used to calculate critical properties for arbitrary d.

The calculation of dynamic and transport properties in the quantum critical regime at finite temperatures turns out to be significantly more complicated. Below d_c^+, dynamic properties are dominated by relaxation processes at frequencies $\omega \ll T$, and in this regime the ϵ expansion

fails. However, considerable progress can be made by applying quasiclassical techniques, where the excitations above the ground state can be described by quasiclassical waves or particles [3]. For transport calculations, quasiclassical methods are not sufficient, and a quantum-mechanical treatment using, e.g., a full quantum Boltzmann equation, is necessary. These techniques have been applied to a number of models [3], but many issues including the influence of disorder remain subject for future work. In contrast, above d_c^+ perturbation theory is useful in many cases, and the presence of quasiparticles allows us to analyse transport using a quasiclassical Boltzmann equation.

Beyond perturbative approaches, various numerical techniques have been employed to investigate quantum phase transitions, some of which closely follow the general idea of renormalization. One example is the numerical RG (NRG) method for quantum impurity problems, proposed by Wilson [22].

2.8. Example: the transverse-field Ising model

In this section, we want to illustrate the general ideas presented above by discussing the Ising model in a transverse field, which displays a paradigmatic example of a quantum phase transition. An experimental realization of this model can be found in the low-temperature magnetic properties of $LiHoF_4$. This material is an ionic crystal, and at sufficiently low temperatures the only magnetic degrees of freedom are the spins of the holmium atoms. They have an easy axis, i.e. they prefer to point up or down with respect to a certain crystal axis. Therefore they can be represented by Ising spin variables. Spins at different holmium atoms interact via a dipolar interaction. Without an external magnetic field the ground state is a fully polarized ferromagnet.

In 1996 Bitko *et al* [5] measured the magnetic properties of $LiHoF_4$ as a function of temperature and a magnetic field that was applied perpendicular to the preferred spin orientation. The resulting phase diagram is shown in figure 2. A minimal microscopic model for the relevant magnetic degrees of freedom is the Ising model in a transverse field. Choosing the z-axis to be the spin easy axis, the Hamiltonian is given by

$$H = -J \sum_{\langle ij \rangle} S_i^z S_j^z - h \sum_i S_i^x. \tag{21}$$

Here S_i^z and S_i^x are the z and x components of the holmium spin at lattice site i, respectively. The first term describes the ferromagnetic interaction between the spins, while the second

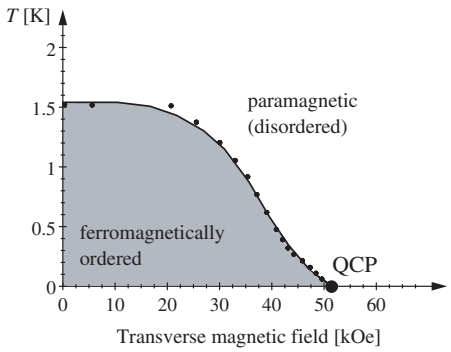

Figure 2. Magnetic phase diagram of $LiHoF_4$ (after [5]). The ordered phase breaks a Z_2 symmetry of the Hamiltonian and is bounded by a line of finite-temperature phase transitions. This line terminates in the QCP, where ferromagnetic order is destroyed solely by quantum fluctuations.

term is the transverse magnetic field. For zero field, $h = 0$, the model reduces to the well-known classical Ising model, with a ferromagnetic ground state. With increasing temperature, thermal fluctuations of the spins will reduce the total magnetization, which will eventually vanish at the critical temperature (about 1.5 K for $LiHoF_4$) above which the system becomes paramagnetic. The resulting transition is a continuous classical phase transition caused by thermal fluctuations.

Let us now consider the influence of the transverse magnetic field. Rewriting $hS_i^x = h/2(S_i^+ + S_i^-)$, with S_i^+ and S_i^- being spin flip operators at site i, it is clear that the transverse field will cause spin flips that are precisely the quantum fluctuations discussed before. If the transverse field becomes larger than some critical field, h_c (about 50 kOe in $LiHoF_4$), they will destroy the ferromagnetic long-range order in the system even at zero temperature. This transition is a continuous quantum phase transition driven exclusively by quantum fluctuations; the phase diagram is of the class shown in figure 1(*b*).

For the transverse-field Ising model, the quantum–classical mapping discussed in section 2.3 can be easily demonstrated at a microscopic level. Consider a one-dimensional classical Ising chain with the Hamiltonian

$$H_{\mathrm{cl}} = -J \sum_{i=1}^{N} S_i^z S_{i+1}^z. \tag{22}$$

Its partition function is given by

$$Z = \mathrm{Tr}\, \mathrm{e}^{-H_{\mathrm{cl}}/T} = \mathrm{Tr} \exp\left(\frac{J \sum_{i=1}^{N} S_i^z S_{i+1}^z}{T} \right) = \mathrm{Tr} \prod_{i=1}^{N} M_{i,i+1}, \tag{23}$$

where $\boldsymbol{M}$ is the so-called transfer matrix. It can be represented as

$$\boldsymbol{M} = \begin{pmatrix} \mathrm{e}^{J/T} & \mathrm{e}^{-J/T} \\ \mathrm{e}^{-J/T} & \mathrm{e}^{J/T} \end{pmatrix} = \mathrm{e}^{J/T}(1 + \mathrm{e}^{-2J/T} S^x) \approx \exp\left(\frac{J}{T} + \mathrm{e}^{-2J/T} S^x \right).$$

Except for a multiplicative constant the partition function of the classical Ising chain has the same form as that of a single quantum spin in a transverse field, $H_{\mathrm{Q}} = -hS^x$, which can be written as

$$Z = \mathrm{Tr}\, \mathrm{e}^{-H_{\mathrm{Q}}/T_{\mathrm{Q}}} = \mathrm{Tr}\, \mathrm{e}^{hS^x/T_{\mathrm{Q}}} = \mathrm{Tr} \prod_{i=1}^{N} \mathrm{e}^{hS^x/(T_{\mathrm{Q}}N)}. \tag{24}$$

Thus, a single quantum spin can be mapped onto a classical Ising chain. Under this mapping, the classical temperature is related to a coupling constant in the quantum model, $h \equiv \mathrm{e}^{-2J/T}$ (being the inverse correlation length of the classical problem), and the classical system size, N, maps onto the inverse of the quantum temperature, T_{Q}. These considerations can easily be generalized to a d-dimensional transverse-field (quantum) Ising model that can be mapped onto a $(d + 1)$-dimensional classical Ising model. Consequently, the dynamic exponent is $z = 1$ here.

3. Bulk quantum phase transitions

In this section we will review a number of classes of quantum phase transitions occuring in condensed matter systems. We will focus our attention on continuous quantum phase transitions, which are characterized by diverging correlation lengths and times.

The continuous transitions discussed here are so-called bulk transitions, meaning that degrees of freedom of the whole sample become critical at the transition point, as is the case

with most familiar phase transitions. This implies that the singular part of free energy of the system scales as L^d, where L is the linear spatial extension of the system and d the space dimensionality. In section 4 we will discuss so-called boundary transitions where only a subset of the available degrees of freedom becomes critical.

Most of the following considerations will deal with 'clean' systems, where translational invariance is unbroken and quenched disorder is absent. The interplay between disorder and criticality is a notoriously difficult issue—even in classical systems—and only understood in some specific models to date; we will touch upon this issue in section 3.3.

3.1. Quantum phase transitions and fermions

Quantum critical behaviour depends crucially on whether order parameter fluctuations can couple to low-energy fermionic excitations (or, more generally, to other non-critical soft modes of the system). In the absence of gapless fermions the order parameter fluctuations are the only low-energy excitations in the vicinity of the critical point, and the critical theory can be formulated in terms of the order parameter alone. Technically, the step of integrating out the fermions from the action describing the interacting electron system does not lead to any divergences.

Critical dynamics can be fundamentally changed if order parameter fluctuations couple to low-energy fermions, as are present in metals. Here, integrating out fermions can lead to divergences. In some cases, it is believed that a formulation of a critical theory for the order parameter alone is still possible; however, the presence of low-energy fermions leads to non-analytic terms in the effective order parameter theory—an example is the Landau damping of critical magnetic fluctuations in metals.

In the following, we specialize the discussion to conventional order parameters that can be written in terms of local fermion operators and carry a certain momentum, $\boldsymbol{Q}$. In a translational invariant system, momentum conservation dictates that an effective coupling between order parameter and fermionic excitations is only possible if the characteristic wavevector, $\boldsymbol{Q}$, of the order parameter connects Fermi surface points, as fermions can be scattered off order parameter fluctuations acquiring a momentum change of $\boldsymbol{Q}$. Four cases have to be distinguished, characterizing the order parameter momentum $\boldsymbol{Q}$: (i) If the order parameter has zero total momentum, as for a ferromagnet, then it couples to particle–hole pairs at the whole Fermi surface. We will further discuss this case in section 3.2.3. For an order parameter with finite momentum $\boldsymbol{Q}$, the remaining cases are the following. (ii) $\boldsymbol{Q}$ cannot connect points on the Fermi surface. Then low-energy fermions are scattered into states with higher energy, and perturbation theory in the corresponding coupling is convergent and only gives a renormalization of parameters. Thus, the critical behaviour is the same as in insulators. (iii) $\boldsymbol{Q}$ connects a $(d-2)$-dimensional set of points, i.e. lines in $d=3$ or discrete points in $d=2$. This leads to damping of the order parameter modes due to the decay into particle–hole pairs. At least in $d=3$ it is believed that this effect can be fully captured by a Landau damping term in the effective action, which increases the dynamic critical exponent; explicit examples are in section 3.2.3. (iv) For so-called perfect nesting, $\boldsymbol{Q}$ can connect whole parts of the Fermi surface, and then a transition generically occurs at infinitely small coupling.

An effective coupling between order parameter fluctuations and low-energy fermions can also be present in unconventional superconductors that have point or line nodes in their gap function, because then a Fermi surface still exists, although it is no longer $(d-1)$-dimensional. A particular example is a two-dimensional d-wave superconductor (see section 3.2.4). Similar considerations apply to semimetals.

For unconventional order parameters, e.g. for glassy order or topological order, the situation is less clear. It has been proposed that fluctuations of these order parameters can couple to fermions on the entire Brillouin zone, leading to various scenarios of 'local criticality'.

In general, a critical point involving both low-energy order parameter and fermionic modes can be expected to display two timescales, because order parameter fluctuations can relax both via (damped) order parameter modes and via fermions. Consequently, the critical theory should be characterized by two dynamic critical exponents [23]. A proper RG analysis of such a theory, keeping both low-energy degrees of freedom, has so far only been carried out for the ferromagnetic transition [24].

3.2. Phase transitions with conventional order parameters

This section describes the physics of continuous quantum phase transitions with local order parameters, involving, e.g., spin, charge, Peierls, or phase order. In space dimensions larger than the classical lower-critical dimension (see section 2.6), those transitions are zero-temperature endpoints of a line of classical phase transitions (figure 1(*b*)).

3.2.1. Order parameters. Many order parameters can be expressed as an expectation value of combinations of particle creation and annihilation operators that are local in space and time. The correlation functions of the so-defined local operator, $\mathcal{O}(\boldsymbol{R}_i, t)$, do not decay to zero in the long-distance limit in the ordered phase (long-range order). As the local quantity can oscillate in space, like the magnetization in an antiferromagnet, the order parameter $\phi(\boldsymbol{R}_i)$ is usually defined as the expectation value of $\mathcal{O}$ with the microscopic oscillations removed,

$$\langle \mathcal{O}(\boldsymbol{R}_i)\rangle = \mathrm{Re}[\mathrm{e}^{\mathrm{i}\boldsymbol{Q}\cdot\boldsymbol{R}_i}\phi(\boldsymbol{R}_i)] \tag{25}$$

and $\boldsymbol{Q}$ is the ordering wavevector or characteristic momentum. Sufficiently close to the ordering transition, $\phi(\boldsymbol{R}_i)$ is now slowly varying in space, and can be replaced by a continuum field $\phi(\boldsymbol{r})$. In a path integral description, we then arrive at a bosonic field, ϕ, carrying momentum $\boldsymbol{Q}$.

The order parameter can have multiple components, i.e. be a spinor, vector, or tensor, and the underlying microscopics then defines the symmetry properties. The symmetry in turn determines the allowed terms in the low-energy action and thus the universality class. It also decides about the existence of low-energy modes: an ordered phase that breaks a continuous symmetry supports Goldstone modes. In addition, the order parameter can carry charge, e.g. if it describes particle–particle rather than particle–hole pairing; the presence of long-range Coulomb interactions can then change the nature of both the collective modes and the transition.

We list a few common examples for order parameters below. For density waves, the number of components is $N = 1$, and the density oscillates around its average value as

$$\langle \rho(\boldsymbol{r}, \tau)\rangle = \rho_{\mathrm{avg}} + \mathrm{Re}[\mathrm{e}^{\mathrm{i}\boldsymbol{Q}_\mathrm{c}\cdot\boldsymbol{r}}\phi_\mathrm{c}(\boldsymbol{r}, \tau)]. \tag{26}$$

Similar scalar or Ising order parameters also occur, e.g. for alloy ordering and for Peierls transitions—in the latter the system undergoes a spontaneous doubling of the unit cell, induced for instance by strong electron–phonon or spin–spin interactions. For SDWs, we have a vector order parameter, $N = 3$ and $\alpha = x, y, z$, and the spin density modulation is given by

$$\langle S_\alpha(\boldsymbol{r}, \tau)\rangle = \mathrm{Re}[\mathrm{e}^{\mathrm{i}\boldsymbol{Q}_\mathrm{s}\cdot\boldsymbol{r}}\phi_{\mathrm{s}\alpha}(\boldsymbol{r}, \tau)]. \tag{27}$$

Here, $\boldsymbol{Q}_\mathrm{s} = 0$ describes a ferromagnet. In the presence of strong spin anisotropies, fluctuations in some directions can be frozen out at low energies, then leading to magnetic theories with

$N = 1$ or 2. XY rotor models ($N = 2$) can also represent phase variables, appropriate, e.g. for phase fluctuations in superconductors.

Interestingly, ϕ in equations (26) and (27) is real only for the cases $\boldsymbol{Q} = 0$ and $\boldsymbol{Q} = (\pi, \pi, \ldots)$ (assuming a hypercubic lattice with unit spacing); otherwise ϕ can be complex, with the phase describing a sliding degree of freedom of the density wave; this phase takes discrete values for commensurate wavevectors. In the magnetic case, both collinear and non-collinear SDWs can be described by equation (27) [25]:

$$\begin{aligned} &\text{collinear: } \phi_{s\alpha} = e^{i\Theta} n_\alpha \text{ with } n_\alpha \text{ real,} \\ &\text{spiral: } \phi_{s\alpha} = n_{1\alpha} + i n_{2\alpha} \text{ with } n_{1,2\alpha} \text{ real and } n_{1\alpha} n_{2\alpha} = 0. \end{aligned} \tag{28}$$

We remind the reader that in spin systems Berry phases are important, which can render the analysis in terms of a slowly varying order parameter alone invalid.

Further interesting order parameters are those with an unconventional symmetry; for fermion bilinears this implies that different parts of the Fermi surface contribute with different weights or signs. Examples are superconductors with p, d, or higher angular momentum pairing symmetries. Also, particle–hole pairing of unconventional symmetry is possible; in the charge channel this can be understood as deformation of the Fermi surface leading to 'nematic' states—the transition of a Fermi liquid into such a state is also known as Pomeranchuk instability. While most of the listed cases have wavevector $\boldsymbol{Q} = 0$, finite $\boldsymbol{Q}$ cases are possible as well, an example being the so-called d-density wave or staggered flux order [26], with $\boldsymbol{Q} = (\pi, \pi)$.

3.2.2. Insulators. The simplest quantum-phase transitions are those where the order parameter fluctuations do not couple to low-energy fermionic excitations—this is generically the case in insulators where the gap to charge excitations is large.

Then, it is sufficient to consider a theory of the order parameter fluctuations alone. In most cases, the appropriate continuum theory takes the form of a ϕ^4 theory (17) described in section 2.5, with a dynamic critical exponent, $z = 1$. For clean systems, results for static quantities at $T = 0$ can be obtained from the corresponding classical transition via the quantum–classical mapping. Most critical properties of such transitions are well understood and can be found in textbooks [11, 12]; we will not describe them further here. In contrast, real-time dynamics and transport, in particular at finite temperatures, cannot be easily extracted from the classical results, and are demanding subjects of current research [3]. For disordered systems a number of complications arise, described in section 3.3, and only relatively few results are available.

3.2.3. Metals: non-Fermi liquid behaviour. Fermi liquids in space dimensions $d \geqslant 2$ can display ground-state instabilities towards states with order parameters described in section 3.2.1, which are of considerable practical interest. In most cases, fermionic low-energy modes couple to the order parameter fluctuations; many aspects of the resulting theories are not fully understood to date. In $d \geqslant 2$ the quantum critical theories are then above their upper-critical dimension; therefore non-universal features abound, and microscopic details like the Fermi surface topology become important. A unified picture of these transitions is not yet available.

The investigation of quantum phase transitions in Fermi liquids was pioneered by Hertz [27], who studied the ferromagnetic transition by a RG method. Millis [28] considerably extended this work and computed finite-temperature crossover functions for several magnetic transitions. The theoretical approach (commonly called Hertz–Millis theory) proceeds by

integrating out the fermions from the full interacting theory, keeping only the low-energy order parameter fluctuations in the theory. Although this is a formally exact step, the coefficients of the resulting action will in general be non-local in space and time because the fermionic excitations are gapless. Assuming that the action can be expanded in powers and gradients of the order parameter field ϕ and assuming that it is permissible to truncate such an expansion, one obtains

$$\mathcal{S} = \int \frac{d^d k}{(2\pi)^d} T \sum_{\omega_n} \frac{1}{2}[k^2 + \gamma|\omega_n| + r]|\phi_\alpha(k, \omega_n)|^2 + \frac{g_0}{4!} \int d^d x \, \mathrm{d}\tau (\phi_\alpha^2(x, \tau))^2, \tag{29}$$

for the case that the ordering wavevector $\boldsymbol{Q}$ connects a $(d-2)$-dimensional set of points of the Fermi surface. Compared with the usual ϕ^4 theory, the dynamical term is now replaced by $|\omega_n|$, describing the Landau damping of the order parameter fluctuations, i.e. the possibility to decay into particle–hole pairs. The theory (29) has the dynamic exponent $z = 2$; for the case of a ferromagnet ($\boldsymbol{Q} = 0$) the damping term gets replaced by $|\omega_n/k|$, and hence $z = 3$. Note that the fermionic gap, which occurs in the ordered phase near the momenta connected by $\boldsymbol{Q}$, is not captured by (29), and therefore this action is not to be taken seriously at $r < 0$, $T = 0$ [3].

The type of quantum critical behaviour within Hertz–Millis theory [28] is dictated by the fact that the interaction term is formally irrelevant above the upper-critical dimension, and therefore only (singular) corrections to a Gaussian theory emerge. For example, the specific heat of the three-dimensional antiferromagnet behaves as $C/T = \gamma + A\sqrt{T}$ in the quantum critical region; in other words, the specific heat coefficient, γ, of the Fermi liquid does not diverge upon approaching the quantum phase transition.

Subsequent theoretical work has indicated that the above assumption of a regular gradient expansion of the action breaks down in a number of important cases. In the antiferromagnet case, an analysis of the spin–fermion model has indicated that the Hertz–Millis theory is invalid in $d = 2$ dimensions [29]. For the ferromagnetic transition, it has been shown that non-analytic terms in the spin susceptibility of a usual Fermi liquid lead to corresponding corrections in the effective order parameter theory [19], which drastically modify the critical behaviour. Notably, the resulting interaction terms are non-local, and the explicit form of the four-point vertex is not known, rendering explicit calculations very difficult in this approach. Clearly, an improved theory should be local and should explicitly keep both the order parameter fluctuations and the low-energy fermionic modes, making manifest the presence of two timescales in the effective theory. Such a calculation has been recently performed for the ferromagnetic transition in metals. (In an unconventional superconductor, the situation is somewhat simpler due to the absence of a full Fermi surface, and both order parameter and fermionic modes can be kept, see section 3.2.4.) We briefly describe the results for the ferromagnetic transition [24]: in a clean metal with $1 < d < 3$ the singular behaviour of the Fermi liquid destabilizes any continuous transition with $z = 3$, and therefore only a first-order transition to a ferromagnetic state or a $z = 2$ transition to a state with spiral order appear possible. In $d = 3$ the conclusions are similar; however, the corrections to the $z = 3$ critical point are only logarithmic, and in certain parameter regimes a continuous transition to a ferromagnetic state may be restored. In the disordered case, i.e. for diffusive spin dynamics, it was found that the $z = 4$ fixed point of Hertz is unstable, and instead a new transition with logarithmic corrections to a Gaussian fixed point with $z = d$ occurs.

On the application side, itinerant ferromagnetic transitions have been found in MnSi and other intermetallic compounds; in many cases those transitions become first order at low temperatures, which appears consistent with the theoretical findings. Antiferromagnetic transitions appear in both transition-metal and rare-earth compounds. Great interest has been

focused on the normal-state properties of the high-temperature superconductors, where simple square-lattice antiferromagnetism as well as collinear spin and associated CDWs ('stripes') have been detected [30–33]. Those order parameters apparently coexist and/or compete with d-wave superconductivity at low temperatures. Also, phase transitions involving circulating currents have been proposed to explain the unusual normal-state properties of high-T_c cuprates ([26], [34] and references therein).

Much experimental and theoretical work has been performed on heavy-fermion compounds. A well-studied compound is $CeCu_{6-x}Au_x$, which displays a transition between a heavy Fermi liquid phase and an antiferromagnetic metallic phase at $x = 0.1$. Interestingly, at the transition the specific heat coefficient diverges as $C/T \propto \ln T$, and neutron scattering indicates ω/T scaling in the response functions [35]. However, such scaling is only expected below the upper-critical dimension (see section 2.6), and is clearly at odds with the Hertz–Millis approach. Some proposals have been made to resolve this inconsistency, relating the observed quantum critical behaviour to the breakdown of Kondo screening [36–38]. In [37], a theory of 'local' critical behaviour has been proposed in the spirit of the dynamical mean-field approach [39]; however, non-trivial behaviour emerges here only for two-dimensional systems. A different approach [38] has associated the suppression of Kondo screening with the emergence of a non-magnetic 'fractionalized Fermi liquid' phase, obtained by suppressing magnetic order in the regime of weak Kondo screening (see also section 3.6.2).

3.2.4. Superconductors. It is conceivable that a quantum phase transition occurs with superconductivity being present on both sides including the transition point. The main difference from the metallic case discussed earlier is that low-energy fermions are gapped due to the presence of the superconducting gap. Then, in general the order parameters fluctuations are undamped, and the phase transitions are in the same universality class as the ones in insulators.

However, in unconventional superconductors showing gapless points or lines in momentum space (called nodal points in the following), damping can still occur. An effective coupling between order parameter fluctuation and fermions is only present if the wavevector, $\boldsymbol{Q}$, of the order parameter fluctuations does connect two nodal points (see section 3.1). Those special cases are ideally treated in a theory that keeps both order parameter and fermionic excitations, and examples have been considered in [40, 41]. Candidate transitions are those with a particular (fine-tuned) finite wavevector, $\boldsymbol{Q}$, like SDWs or CDWs, and transitions with $\boldsymbol{Q} = 0$ that do not require any fine tuning. Examples in the latter class are particle–hole pairing transitions that lead to 'nematic' states, and transitions involving the onset of secondary superconducting pairing [41]. Note that for these transitions the onset of the secondary pairing occurs at a finite value of the corresponding coupling because the density of states (DOS) in the background superconducting state vanishes at the Fermi level.

We briefly sketch the theory of the transition between two superconducting states with $d_{x^2-y^2}$ and $d_{x^2-y^2} + \mathrm{i}d_{xy}$ pairing symmetry [41]—this is one of the simplest models where both order parameter fluctuations and low-energy fermionic excitations can be treated on an equal footing. Importantly, the fluctuations of the secondary d_{xy} order parameter are represented by an Ising field (ϕ), because the fluctuations of its phase relative to the background d-wave pairing are massive. Thus we simply have

$$\mathcal{S}_\phi = \int d^2x \, \mathrm{d}\tau \left[\frac{1}{2}(\partial_\tau \phi)^2 + \frac{c^2}{2}(\nabla_x \phi)^2 + \frac{r}{2}\phi^2 + \frac{g_0}{4!}\phi^4 \right], \tag{30}$$

as in equation (17). We explicitly include the low-energy fermions that have a linear spectrum; for one pair of nodes their action can be written as

$$\mathcal{S}_{\Psi 1} = \int \frac{d^2k}{(2\pi)^2} T \sum_{\omega_n} \Psi^\dagger_{1a}(-\mathrm{i}\omega_n + v_\mathrm{F} k_x \tau^z + v_\Delta k_y \tau^x)\Psi_{1a}. \tag{31}$$

Here, $\Psi_{1a} = (f_{1a}, \varepsilon_{ab} f^\dagger_{3b})$ is a Nambu spinor of fermions from opposite nodes (1 and 3) of the d-wave superconductor, τ^α are Pauli matrices that act in the fermionic particle–hole space, $k_{x,y}$ measure the wavevector from the nodal points and have been rotated by 45° from $q_{x,y}$ co-ordinates, and v_F, v_Δ are velocities. (An analogous term describes the nodes 2 and 4.) The full action is then $\mathcal{S} = \mathcal{S}_\phi + \mathcal{S}_{\Psi 1} + \mathcal{S}_{\Psi 2} + \mathcal{S}_{\Psi\phi}$, where the final term in the action, $S_{\Psi\phi}$, couples the bosonic and fermionic degrees of freedom:

$$S_{\Psi\phi} = \int d^2x \, \mathrm{d}\tau [\lambda_0 \phi (\Psi^\dagger_{1a} M_1 \Psi_{1a} + \Psi^\dagger_{2a} M_2 \Psi_{2a})], \tag{32}$$

where $M_{1,2}$ are now specific for the secondary order parameter considered, and for d_{xy} pairing we have $M_1 = \tau^y$, $M_2 = -\tau^y$ [41]. This theory can be analysed by perturbative RG together with ϵ expansion in standard fashion. The resulting transition has dynamical exponent $z = 1$, and the ordered phase breaks a Z_2 symmetry. However, the transition is not in the Ising universality class due to the coupling to the fermions. An explicit calculation of the boson propagator shows that it contains non-analytic terms in both k and ω that are different from simple Landau damping. The sketched theory has been proposed to describe the strong damping of nodal fermions in cuprates below the superconducting T_c [41].

3.3. Quantum phase transitions and disorder

In application to real systems the influence of static or quenched disorder on the properties of a quantum phase transition is an important aspect. Remarkably, the effect of disorder is not completely understood even for classical phase transitions.

In a theoretical description, quenched disorder can occur in different ways: on a microscopic level, e.g., random site energies, bond couplings, or randomly distributed scattering centres are possible. In an order parameter field theory, disorder usually translates into a random mass term for the order parameter fluctuations. Importantly, applying the quantum–classical mapping (section 2.3) to a quantum problem with quenched disorder leads to a $(d + z)$-dimensional field theory with strongly anisotropic correlated disorder because the disorder is frozen in the time direction. In some cases lattice effects not captured by the field theory can be important; this applies, e.g., to all types of percolation problems. Moreover, disordering a quantum model can lead to random Berry phase terms that have no classical analogue, an example is diluted Heisenberg antiferromagnets.

A basis for the discussion of the effect of disorder on continuous transitions is given by the Harris criterion [42, 43], which states that if the correlation length exponent, ν, of a given phase transition obeys the inequality $\nu \geqslant 2/d$, with d the space dimensionality of the system, then the critical behaviour is unaffected by quenched disorder. In the opposite case, $\nu < 2/d$, the disorder modifies the critical behaviour, leading (i) to a new critical point that has a correlation length exponent, $\nu \geqslant 2/d$, and is thus stable, or (ii) to an unconventional critical point where the usual classification in terms of power-law critical exponents loses its meaning, or (iii) to the destruction of a sharp phase transition. The first possibility is realized in the conventional theory of random-T_c classical ferromagnets [44], and the second one is probably realized in classical ferromagnets in a random field [45]. The third one has occasionally been attributed to the exactly solved McCoy–Wu model [46]. This is misleading, however, as has

been emphasized in [49]; there is a sharp, albeit unorthodox, transition in that model, and it thus belongs to category (ii).

For first-order transitions, Imry and Wortis [47] have proposed a criterion stating that below a certain critical dimension (which is usually 2) the transition will be significantly rounded due to domain formation. The question of whether the possibly resulting continuous transition shows universal scaling is not settled [48].

Independent of the question of if and how the critical behaviour is affected, disorder leads to very interesting phenomena as a phase transition is approached. Disorder in classical systems generically decreases the critical temperature, T_c, from its clean value, T_c^0. In the temperature region $T_c < T < T_c^0$, the system does not display global order, but in an infinite system one will find arbitrarily large regions that are devoid of impurities, and hence show local order, with a small but non-zero probability that usually decreases exponentially with the size of the region. These static disorder fluctuations are known as 'rare regions', and the order parameter fluctuations induced by them as 'local moments' (LMs) or 'instantons'. Since they are weakly coupled, and flipping them requires changing the order parameter in a whole region, the LMs have very slow dynamics. Griffiths [50] was the first to show that they lead to a non-analytic free energy everywhere in the region $T_c < T < T_c^0$, which is known as the Griffiths phase, or, more appropriately, the Griffiths region. In generic classical systems this is a weak effect, since the singularity in the free energy is only an essential one. (An important exception is the McCoy–Wu model [46].)

Turning now to quantum phase transitions, it is expected that disorder has a stronger effect compared with the classical case due to the disorder correlations in time direction. Consequently, the Harris criterion is still given by $\nu < 2/d$ (not $d + z$). A prototypical and well-studied model is the quantum Ising chain in a transverse random field, investigated by Fisher [49] and others, where the phase transition is controlled by a so-called infinite-randomness fixed point, characterized by a wide distribution of couplings and activated rather than power-law critical behaviour. The Griffiths singularities are also enhanced compared with the classical case: a number of observables display power-law singularities with continuously varying exponents over a finite parameter region in the disordered phase. Numerical simulations [53] suggest that random-singlet phases and activated criticality may not be restricted to one-dimensional systems, raising the possibility that exotic critical behaviour dominated by rare regions may be common to certain quenched-disorder quantum systems, in particular those with Ising symmetry. Recent investigations of two-dimensional diluted bilayer antiferromagnets with Heisenberg symmetry indicate conventional critical behaviour, and in addition an interesting interplay of quantum and geometric criticality at the percolation threshold [51].

All the examples mentioned so far display undamped order parameter dynamics ($z = 1$ in the clean system). In contrast, in itinerant electron systems the dynamics is overdamped due to the coupling to fermions ($z > 1$ in the clean limit, see sections 3.1 and 3.2.3), which also changes the behaviour upon introduction of disorder. It has been shown recently that for Ising order parameter symmetry and overdamped dynamics a continuous transition is always rounded due to the presence of ordered islands arising from a $1/r^2$ interaction in the effective classical model [52]. For continuous symmetries it is likely that a sharp transition survives. A prototype example is the disordered itinerant antiferromagnet, where it has been shown that a finite-disorder fixed point is destabilized by the effects of rare regions. The RG indicates run-away flow to large disorder, and definite conclusions regarding the transition cannot be drawn [54]. In the context of heavy-fermion compounds, it has been suggested that non-Fermi liquid behaviour can occur in the quantum Griffiths region of a disordered Kondo lattice model [55].

Systems which are dominated by disorder and frustration can have a variety of new stable phases not known from clean systems, e.g. spin or charge glasses and various types of infinite-randomness phases. Associated phase transitions then belong to new universality classes, an interesting example being the quantum spin glass transition, i.e. the $T = 0$ transition between a paramagnet and a spin glass [3]. Such transitions may be relevant for certain strongly disordered heavy-fermion compounds, but speculations in the context of high-T_c superconductivity have also been put forward [56].

3.4. Metal–insulator transitions

Metal–insulator transitions are a particularly fascinating and only incompletely understood class of quantum phase transitions. Conceptually, one distinguishes between transitions in models of non-interacting electrons, arising solely from lattice effects, and transitions of interacting electrons. Examples in the first class are band or Peierls metal–insulator transitions, as well as the disorder-driven Anderson transition. The prominent example in the second class is the Mott transition of clean interacting electrons. At the Anderson transition, the electronic charge diffusivity, D, is driven to zero by quenched disorder, while the thermodynamic properties do not show critical behaviour. In contrast, at the Mott transition the thermodynamic density susceptibility, $\partial n/\partial\mu$, vanishes due to electron–electron interaction effects. In either case, the conductivity, $\sigma = (\partial n/\partial\mu)D$, vanishes at the metal–insulator transition. It is worth emphasizing that a sharp distinction between metal and insulator is possible only at $T = 0$; in some cases, a first-order finite-temperature transition between a 'good' and a 'bad' metal can occur.

Let us briefly discuss the disorder-driven metal–insulator transition. Introducing quenched disorder into a metallic system, e.g. by adding impurity atoms, can change the nature of the electronic states from spatially extended to localized [57]. This localization transition of disordered non-interacting electrons, the Anderson transition, is comparatively well understood (see [58]). The scaling theory of localization [59] is based on the assumption of hyperscaling and predicts that in the absence of spin–orbit coupling or magnetic fields all states are localized in one and two space dimensions for arbitrarily weak disorder. Thus, no true metallic phase exists for $d = 1, 2$. In contrast, in three dimensions there is a phase transition from extended states for weak disorder to localized states for strong disorder. These results of the scaling theory are in agreement with large-scale computer simulations of non-interacting disordered electrons. The effect of weak disorder can be captured by perturbation theory, leading to the well-known 'weak-localization' quantum corrections to the conductivity, which are divergent in $d = 1, 2$. A field-theoretic description of the Anderson transition has been pioneered by Wegner [60]. Starting from electrons in a random potential, the disorder average is performed using the Replica trick, and the arising interaction terms can be decoupled using complex matrix fields. The theory then takes the form of a non-linear sigma model in terms of these matrix fields; it has been subsequently analysed at the saddle-point level and by RG methods, with results consistent with the scaling theory [21].

A different limiting case is the interaction-driven Mott transition of clean electrons that can occur at commensurate band fillings. The most studied model showing such a transition is the one-band Hubbard model, with the Hamiltonian

$$H = -\sum_{\langle ij\rangle\sigma} t_{ij}(c^{\dagger}_{i\sigma}c_{j\sigma} + c^{\dagger}_{j\sigma}c_{i\sigma}) + U\sum_{i} n_{i\uparrow}n_{i\downarrow}, \tag{33}$$

defined on a regular lattice, with hopping energies t_{ij} and an on-site Coulomb repulsion U. At half filling, the system is metallic at $U = 0$, but insulating at $U \to \infty$ because a large U prevents

doubly occupied sites and thus completely suppresses hopping. In general, an interaction-driven metal–insulator transition may be accompanied by the occurrence of magnetic order (Mott–Heisenberg transition). In contrast, the transition from a paramagnetic metal to a paramagnetic insulator is termed Mott–Hubbard transition. Non-perturbative techniques are necesssary to analyse the Mott transition because it generically occurs at intermediate coupling (except for perfect nesting situations).

The Hubbard model (33), both at and away from half-filling, has been extensively studied in the context of high-temperature superconductivity, and a plethora of phases have been proposed as a function of parameters and doping. However, many properties of this apparently simple one-band model in two and three dimensions are still under debate, as analytical calculations often have to rely on uncontrolled approximations, and numerical methods are limited to very small system sizes. In one dimension, special techniques have provided a number of exact answers (see [61]). Beyond that, considerable progress has been made in the framework of dynamical mean-field theory (DMFT) [39], which represents a local approximation to the self-energy and becomes exact in the limit of infinite space dimensions. In this approach, the lattice model is mapped onto a quantum impurity model supplemented by a self-consistency condition. Extensive numerical studies have established that the $T = 0$ Mott transition in the DMFT limit is characterized by the continuous vanishing of the quasiparticle weight upon increasing U/t; however, the insulator displays a preformed gap, and no dynamic critical behaviour is present [39, 62].

In reality, both Coulomb interaction and disorder are present, and their interplay is poorly understood. The conventional approach to the problem of disordered interacting electrons is based on a perturbative treatment of both disorder and interactions [63, 64]. It leads to a scaling theory and a related field-theoretic formulation of the problem [65], which is a generalization of Wegner's theory for non-interacting electrons [60], and was later investigated in great detail within the framework of the RG (for a review see [21]). One of the main results is that in the absence of external symmetry breaking (spin–orbit coupling or magnetic impurities, or a magnetic field) a phase transition between a normal metal and an insulator only exists in dimensions larger than 2, as was the case for non-interacting electrons. In two dimensions the results of this approach are inconclusive since the RG displays runaway flow to zero disorder but infinite interactions. Furthermore, it has not been investigated so far, whether effects of rare regions (section 3.3) would change the above conclusions about the metal–insulator transition. It is known that local moments tend to form in the vicinity of the transition; however, their role in the critical properties has not been clarified. Conceptually, it is clear that a perturbative approach is not applicable in a regime of strong interactions.

Experimental work on the disorder-driven metal–insulator transition, mostly on doped semiconductors, carried out before 1994 essentially confirmed the existence of a transition in three dimensions [66], while no transition was found in two-dimensional systems. Therefore, it came as a surprise when experiments on Si-MOSFETs [10] revealed indications of a true metal–insulator transition in two dimensions. These experiments have been performed on high-mobility samples with a low carrier density. Therefore, electronic interactions are strong: for an electron density of $10^{11}\,\mathrm{cm}^{-2}$ the typical Coulomb energy is about 10 meV, while the Fermi energy is only about 0.5 meV. Interaction effects are a likely reason for this new behaviour in two dimensions; however, a complete understanding has not yet been obtained. It is not settled whether the observations are associated with a true zero-temperature transition, or whether they represent an intermediate-temperature crossover phenomenon. Recent experiments indicate glassy charge dynamics on both the metallic and the insulating sides of the apparent transition, further pointing to an interesting interplay between disorder and interactions.

A number of ideas developed in the context of the Anderson transition also apply to transitions in quantum Hall systems. In each quantum Hall plateau phase, electrons are localized due to disorder, and the longitudinal $T = 0$ conductivity vanishes. Transitions between different quantum Hall states involve a diverging correlation length and scaling behaviour of the conductivity. In addition to scaling theories, approaches based on quantum tunnelling network models, as first proposed by Chalker and Coddington, have been successful in explaining a number of experimental findings. However, at present the role of electron interactions at the quantum Hall critical points has not been thoroughly clarified. For a full exposure we refer to recent review articles [1, 67].

Summarizing, metal–insulator transitions, in particular those occurring at intermediate or strong interactions, are in the focus of current research activity, and many aspects, including the interplay with lattice effects and magnetism, remain to be understood.

3.5. Superfluid–insulator transitions

Transitions between superfluid and insulating states can, like metal–insulator transitions, be driven by disorder or by strong Coulomb interaction; in the case of a charged superfluid, i.e. a superconductor, applying a magnetic field can also lead to a superconductor–insulator transition. Both the disorder and field-driven transitions have been extensively studied in the context of thin superconducting films. Interaction-driven (Mott) transitions can be realized in Josephson junction arrays where the ratio between the inter-island Josephson coupling and the intra-island Coulomb interaction can be varied [1]. Very recently, clear signatures of a Mott superfluid–insulator transition have been observed in a system of ultracold atoms in an optical lattice [68].

Usually, models of bosons are employed to describe a superfluid. For the disorder-free case with interactions, one is led to the boson Hubbard model, introduced in section 2.5, which contains a tight-binding hopping energy, t, and an on-site repulsion, U. The ground-state phase diagram is well understood: in a plane parametrized by the chemical potential, μ/t, and the ratio t/U, the large-t regime is superfluid, whereas in the small-t regime Mott phases occur where the density is fixed to integer values. The transitions are described by an O(2) rotor model capturing the condensate phase dynamics, provided the density is fixed—this is the case at the tips of the so-called Mott lobes of the phase diagram. Otherwise, the complex condensate density itself is the appropriate order parameter, and the transition is in the dilute Bose gas class [3].

In the presence of disorder, the situation is somewhat more complicated. In addition to the Mott insulator and superfluid phases a Bose glass phase appears that is believed to be insulating. Particular attention has been focused on the two-dimensional case, where the scaling dimension of the conductivity turns out to be zero. Thus, scaling theories predict a universal metallic resistance exactly at the transition point between a superconductor and insulator [1, 69]. An important feature of the theory is the relevance of long-range Coulomb interaction at the transition, which leads to a dynamical critical exponent being unity [69]. A duality description of the two phases, involving bosons and vortices, has been put forward: in the superconducting phase the bosons are condensed and the vortices localized, whereas in the insulating (Bose glass) phase the bosons are localized and the vortices condensed—this corresponds to a superfluid of vortices [70].

While these theories were confirmed by a number of experimental studies, they have been called into question by recent experiments on superconducting films in a field, which suggest the existence of a finite intermediate regime of metallic behaviour. A number of proposals have been put forward, ranging from a metallic Bose glass, or a true Bose metal, to metallicity

produced by the influence of dissipation [71]. Other speculations concern the possible influence of fermionic excitations, which are usually ignored in boson-only models. In this context one has to keep in mind that in two dimensions a fermionic metallic phase is believed to be absent due to weak localization; however, the experimental findings on two-dimensional electron gases mentioned in section 3.4 have called this into question as well. Thus, the fascinating fields of metal–insulator and superconductor–insulator transitions are firmly connected, and the interplay between disorder and interactions remains an important topic of future research.

3.6. Phase transitions involving topological order

Phase transitions can involve the onset of so-called topological order; in this case the ordered state is not characterized by a local order parameter; however, the two phases can be distinguished from their global properties. In many cases, topological order can be rephrased as the suppression of topological defects, either in physical (e.g. spin) or emergent (gauge field) degrees of freedom. The transition from a topologically ordered to a disordered state can be described as the proliferation of topological defects. Topological order occurs in different contexts, e.g. in the quantum Hall effect, in superconductors, and in spin systems; we will describe a few interesting transitions below.

3.6.1. Kosterlitz–Thouless transition. A well-known classical example is the finite-temperature transition of the $d = 2$ XY model, i.e. a model where spins are confined to the x–y plane, which is equivalent to a O(2) rotor model. At high temperatures the spins are disordered with exponentially decaying correlations, whereas at low, non-zero temperatures the spin displays quasilong-range order with power-law correlations. This quasiordered phase has topological vortex excitations that are suppressed at low temperatures; i.e. the density of vortex–antivortex pairs is small. The two phases are separated by a Kosterlitz–Thouless transition at T_{KT}, where vortex pairs unbind upon increasing temperature; the transition is accompanied by a universal jump in the superfluid density. The XY model is of relevance for the phase dynamics of two-dimensional superconductors and has been discussed extensively in the context of underdoped high-temperature superconducting cuprates.

A Kosterlitz–Thouless quantum phase transition occurs at $T = 0$ in the (1+1)-dimensional XY model, or equivalently in the O(2) rotor model in $d = 1$—this follows straightforwardly from the quantum–classical mapping of section 2.3. Technically, the physics is contained in a model of the sine-Gordon type, where the action of a free field describing the phase dynamics is supplemented by a term arising from vortex tunnelling events [3].

The model can be analysed by conventional RG methods; interestingly, formally the same RG equations occur in the context of the Kondo model and will be discussed in section 4.1. The RG analysis shows that the Kosterlitz–Thouless transition does not correspond to a critical, i.e. unstable, fixed point in the RG sense; therefore 'conventional' quantum critical behaviour (as in figure 1) and the corresponding power laws do not occur near the vicinity of the transition point. Connected to that, the Kosterlitz–Thouless transition does not yield a singularity in any derivative of the thermodynamic potential at the transition, and therefore it is sometimes called an infinite-order transition.

3.6.2. Fractionalization transitions. In the context of strongly correlated electron systems in dimensions $d > 1$, phases with 'fractionalized' elementary excitations, carrying quantum numbers different from multiples of those of the electron, have attracted considerable attention in recent years. Fractionalization is usually discussed by recasting the original model into a theory of new (fractionalized) quasiparticles, e.g. spinons and chargons, interacting with each

other through a gauge field: the quasiparticles will carry a gauge charge. A fractionalized phase corresponds to a deconfined phase of the gauge theory; i.e. the effect of the gauge field is weak. In contrast, if the gauge field is confining, the fractionalized quasiparticles are bound at low energies, resulting in excitations with conventional quantum numbers. The fractionalization transition between two such phases corresponds to a confinement–deconfinement transition of a certain gauge theory. The transition can be driven either by the condensation of topological defects of the gauge field or by the condensation of matter (Higgs) fields that are coupled to the gauge field.

The most prominent examples of gauge theories in the context of fractionalization are the ones with Z_2 [72, 73] and U(1) [74] symmetry of the gauge field. Based on early work on the phase diagram of the U(1) gauge theory by Fradkin and Shenker [75], it is believed that Z_2 fractionalization can occur in $d = 2, 3$, whereas U(1) fractionalization can only occur in $d = 3$. The deconfined phases of these theories possess topological order, which is associated with the suppression of topological defects in the gauge field; this order also manifests itself in a topological ground state degeneracy if the system is subjected to periodic boundary conditions.

Fractionalization has been intensively discussed in the context of low-dimensional undoped and doped Mott insulators, with particular focus on high-T_c superconductivity. In fact, Anderson's resonating valence bond state for two-dimensional antiferromagnets [76] is one of the first proposals for a fractionalized spin liquid. A powerful description of such a singlet liquid state is provided by Z_2 gauge theory models [72, 73], see [25] for further discussions. Experimental tests for fractionalization, based on the existence of vortices (so-called visons) in the Z_2 gauge field, have been undertaken, but no topological order has been detected so far in cuprates.

Significant progress has been made in constructing explicit models that show fractionalization; these involve simple models of bosons and fermions on regular lattices [74]. A notable achievement is the demonstration of fractionalization in the triangular lattice quantum dimer model [77]; furthermore, indications for fractionalization have been found in numerical investigations of ring-exchange models on the triangular lattice, and charge fractionalization has been demonstrated in a correlated model on the pyrochlore lattice [78].

Recently, proposals for fractionalized phases in Kondo-lattice models have been put forward [38]. Here, in the presence of strong quantum fluctuations the local moments (LMs) can form a fractionalized spin liquid in a regime where the intermoment interaction dominates over Kondo screening. The topological order protects this spin liquid against small perturbations, and thus the conduction electrons will be essentially decoupled from the LMs. This peculiar paramagnetic phase has been termed a 'fractionalized Fermi liquid', as it displays both Fermi-liquid-like particle–hole excitations and fractionalized spinon excitations, arising from the conduction electron and LM subsystems, respectively. Increasing the Kondo coupling eventually drives the system through a (Higgs) confinement transition into the usual heavy Fermi liquid phase. Approaching from the Fermi liquid side, this zero-temperature transition can be understood as the breakdown of Kondo screening. The quantum critical region of this fractionalization transition displays novel critical behaviour [38] which may be related to experimental findings in heavy-fermion systems like $CeCu_{6-x}Au_x$ [35].

It is clear that fractionalization in $d > 1$ is a fascinating field that can lead to a plethora of new phenomena in condensed matter physics. Although experimental evidence for the occurrence of such phases is lacking to date, we have to keep in mind that the experimental distinction can be very subtle due to the absence of a conventional order parameter; it could very well be the case that fractionalization is realized in recently studied strongly correlated materials. Therefore, further theoretical work predicting properties and proposing stringent tests of fractionalization is called for.

3.7. Competing orders

The physics of competing orders has been a central theme in low-dimensional correlated electron systems over the last years. In particular, in two dimensions extensive studies of microscopic models have shown that a variety of phases compete, and the actual ground state may depend sensitively on details of the model parameters. The interplay of different orders appears crucial for the understanding of the complex phase diagrams of various materials, with high-temperature superconductors being a paradigmatic example.

On the theoretical side, competing orders imply the existence of multiple order parameters. A simple phenomenological description involves a Landau-type theory of coupled order parameter fields, in which the form of the allowed terms follows from symmetry arguments. Let us discuss the case of two order parameters, ϕ_A and ϕ_B, that break different symmetries of the Hamiltonian: then the simplest allowed coupling is usually of the density–density type $|\phi_A|^2|\phi_B|^2$. The Landau theory will generically permit four phases: disordered, pure A, pure B, and coexistence of A and B. Tuning the system between the pure A and pure B phases leads either to two continuous transitions, with a coexistence phase or disordered phase in between, or to a first-order transition between A and B; the occurence of a single continuous transition requires additional fine tuning of parameters in the action.

In the context of high-T_c superconductors, the competition between magnetism and superconductivity has been studied extensively. On the one hand, static magnetism tends to suppress superconductivity, and on the other hand, magnetic fluctuations are believed to mediate pairing (perhaps supplemented by phonons). The intimate relation between antiferromagnetism and d-wave superconductivity has been suggested to arise from an (approximate) higher symmetry of the underlying model, namely an $SO(5)$ symmetry unifying the two-component superconducting and the three-component magnetic order parameters [79]. Other proposals for orders competing and/or coexisting with superconductivity involve charge–stripe order [32, 33], nematic order [80], circulating currents [26, 34], and more exotic orders related, e.g. to spin–charge separation [73].

Recent neutron scattering and scanning tunnelling microscopy (STM) experiments indicate that important competitors of superconductivity are incommensurate spin and associated CDWs. The SDWs correspond to a collinear spin order at wavevectors $\boldsymbol{Q}_{sx} = (\pi \pm \epsilon, \pi)$ and $\boldsymbol{Q}_{sy} = (\pi, \pi \pm \epsilon)$ where ϵ depends on doping. On general symmetry grounds, such a spin order ($\phi_{s\alpha}$) is accompanied by charge order (ϕ_c) at wavevectors $\boldsymbol{Q}_c = 2\boldsymbol{Q}_s$; formally this follows from the existence of a cubic term ($\phi_{s\alpha}^2\phi_c^* + \text{c.c.}$) in the field theory, which is allowed only if $\boldsymbol{Q}_c = 2\boldsymbol{Q}_s$ due to momentum conservation. (Note that CDW order can exist without simultaneous SDW order.) Incommensurate spin and charge orders, coexisting with superconductivity at low T, have been detected in Nd- and Eu-doped $La_{2-x}Sr_xCuO_4$ [30]. A number of other experimental results [81, 82] can also be explained by proximity to a QCP at which spin/charge order disappears: even in optimally doped compounds that show no long-range spin order, a suitable description of the collective spin and charge excitations is given by a theory assuming the vicinity of an ordering transition at lower doping. Then, the additional order parameters are fluctuating [25, 83], and will show up in suitable dynamic measurements. Charge fluctuations can also become static due to impurity pinning, and thus be detectable, e.g. by STM. An applied magnetic field can enhance competing spin/charge fluctuations or even stabilize static SDW/CDW order by suppressing the competing superconductivity due to vortex superflow [84, 25]. Recent STM experiments on optimally doped $Bi_2Sr_2CaCu_2O_{8+x}$ in a magnetic field show that a checkerboard modulation occurs in the local DOS near vortex cores [82] (see figure 3). This supports the idea of competing orders, and a likely explanation is that dynamic collective charge fluctuations are enhanced in the regions of weakened

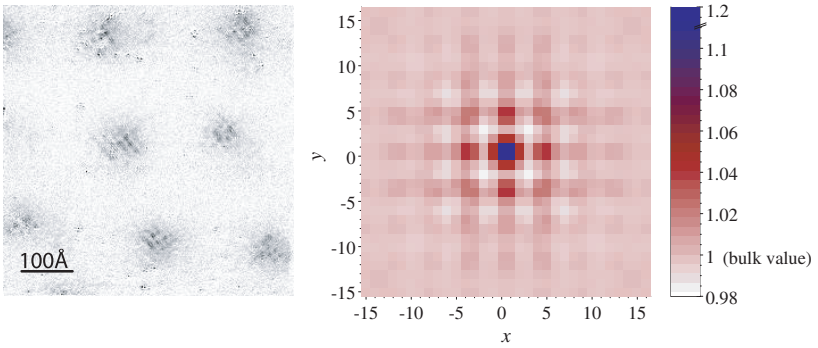

Figure 3. Left: greyscale plot of the local DOS as measured by STM at the surface of $Bi_2Sr_2CaCu_2O_{8+x}$ in a magnetic field of 7 T, integrated over an interval of subgap energies (after [82]). The dark regions can be identified as the locations of vortices. Around each vortex a checkerboard modulation is clearly visible; with the lattice constant being about 3.9 Å for $Bi_2Sr_2CaCu_2O_{8+x}$ the modulation period is found to be four lattice spacings. Right: theoretical computation of the local DOS within a pinning model for the dynamic SDW fluctuations [85]—here the unit of length is the lattice constant. (The crystal axes are rotated by approximately 45° in the left plot.)

superconductivity and pinned by local imperfections, like the vortex cores themselves [85]. A detailed modelling of the energy dependence of the STM signal indicates that it is best described by a checkerboard modulation in microscopic bond rather than site variables [86].

At the microscopic level, the most important aspect of cuprates is that superconductivity is obtained from doping a Mott insulator. The generic phase diagram of doped Mott insulators is not understood to its full extent; however, it is clear that various spin and charge ordered phases, superconductivity, and more exotic phases could be realized. One simple scenario, based on large-N calculations for an extended t–J model, has been put forward in [41]: starting from a paramagnetic Mott insulator with bond order, doping naturally leads to superconducting phases co-existing with bond order, i.e. stripe-like charge density modulations. The resulting phase diagram is reproduced in figure 4. The interplay between superconductivity and bond order has been studied in some detail in [41,86]: the ordering wavevector shows a characteristic evolution with doping, and period-4 structures have been found stable over a significant doping and parameter range. Phase diagrams with related physical ingredients, but some significant differences, appear in [33, 80]. We note that a number of experimental results indicate spin freezing into a glassy state below optimal doping, as has been pointed out by Panagopoulos *et al* [56]—this may be expected in the presence of disorder in a region of the phase diagram where spin ordering occurs in the clean limit.

Besides the high-T_c compounds, numerous other strongly correlated materials display competing orders. Evidence for co-existing antiferromagnetism and superconductivity has also been found in heavy-fermion compounds, e.g. $CePd_2Si_2$, $CeCu_2Si_2$, and $CeIn_3$. However, in these materials the nature of the superconducting state has not been established to date. Other examples are colossal magnetoresistance manganites, ruthenium oxides, and organic conductors of the TMTSF and BEDT-TTF type.

4. Boundary quantum phase transitions

This section is devoted to the special class of boundary phase transitions. Such transitions occur in systems that can be divided into a bulk part with space dimension d and another part

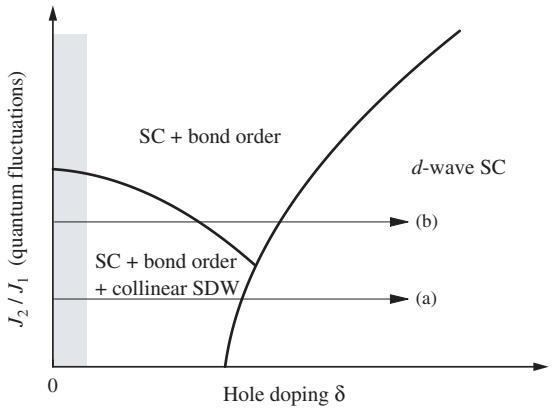

Figure 4. Schematic $T = 0$ phase diagram (after [41, 25]) for the high-temperature superconductors. The vertical axis denotes a parameter that can destroy antiferromagnetic order in the undoped limit, like the ratio of the near-neighbour exchange interactions; the horizontal axis is the hole concentration, δ. The ground state is insulating at a small doping due to Coulomb interactions (shaded). All other phases at finite δ show superconductivity which can coexist with bond/charge order and possibly collinear magnetic order at lower doping. The two arrows (a) and (b) correspond to the possible hole doping evolution of different compounds.

with dimension $d_b < d$—this 'boundary' part can be either a surface or interface, or even a single impurity ($d_b = 0$) embedded into the bulk. At a boundary transition only the boundary degrees of freedom undergo a non-analytic change. At a continuous boundary phase transition, there is a singular part in the free energy that scales as L^{d_b}, where L is the linear dimension of the system.

Boundary transitions have been extensively discussed in the context of surface transitions in magnets [87], where under certain conditions the surface spins can order at a temperature above the bulk ordering temperature. The fascinating aspects of quantum criticality can also be found in boundary transitions. Here, we shall describe a few zero-temperature transitions in quantum impurity systems, which have been of much interest in diverse fields such as unconventional superconductors, heavy fermions, quantum dot systems, and quantum computing.

4.1. Kondo effect in metals and pseudogap Fermi systems

A magnetic impurity spin, $\boldsymbol{S}$, embedded in a bulk system of non-interacting conduction electrons (figure 5(*a*)) can be described by the so-called Kondo Hamiltonian,

$$H = \sum_{k\sigma} \varepsilon_k c^\dagger_{k\sigma} c_{k\sigma} + J_K \boldsymbol{S} \cdot \boldsymbol{s}(0), \tag{34}$$

where $\boldsymbol{s}(0) = \sum_{\boldsymbol{k}\boldsymbol{k}'\boldsymbol{\sigma}\boldsymbol{\sigma}'} c^\dagger_{\boldsymbol{k}\sigma} \boldsymbol{\sigma}_{\sigma\sigma'} c_{\boldsymbol{k}'\sigma'}$ is the conduction electron spin at the impurity site $\boldsymbol{r} = 0$. The Kondo effect in metals, occuring at any positive value of the Kondo coupling, J_K, is by now a well-studied phenomenon in many-body physics. In essence, at low temperatures the conduction electrons and the impurity spin form a collective many-body state with zero total spin. The scattering of the conduction electrons off the impurity gives rise to non-trivial transport behaviour, namely a temperature minimum in the electric resistivity of a metal with dilute magnetic impurities. For small $J_K > 0$, the low-energy physics of an isolated impurity is completely determined by a single energy scale, $k_B T_K$, where T_K is the Kondo temperature. The impurity spin is fully screened by the conduction electrons in the low-temperature limit,

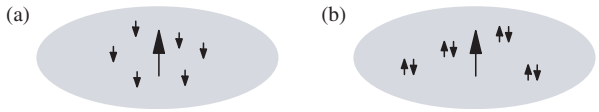

Figure 5. (*a*) Visualization of Kondo screening in metals: an impurity spin is surrounded by conduction electrons with primarily opposite spin. (*b*) Kondo screening in superconductors is suppressed because the low-energy electrons are locked into Cooper pairs. However, for J_K larger than the Cooper pair binding energy screening is again possible—this can be interpreted as Bogoliubov quasiparticles bound locally to the impurity spin.

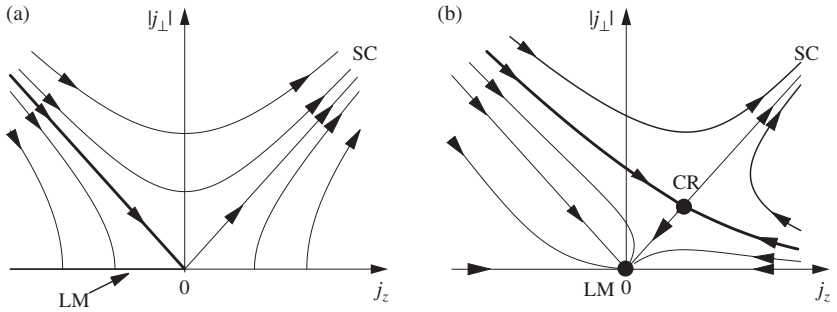

Figure 6. RG flow for the anisotropic Kondo model. The thick lines denote the separatrices corresponding to the phase transitions between local moment (LM) and strong-coupling (SC) behaviour. (*a*) Metallic case, i.e. for a finite bath DOS ρ_0 at the Fermi level. Here the transition is of Kosterlitz–Thouless type. (*b*) Pseudogap case, $\rho(\epsilon) = \rho_0|\epsilon/D|^r$ ($r > 0$), showing a continuous transition with a critical fixed point, CR.

$T \ll T_K$. T_K depends exponentially on the DOS at the Fermi level, $\rho_0 = \rho(\epsilon_F)$, and the Kondo coupling, J_K [88].

For ferromagnetic $J_K < 0$, the physics is different, and no screening occurs. Instead, in the low-temperature limit the impurity spin is effectively decoupled from the conduction band, and contributes a residual entropy of $S_0 = k_B \ln 2$. The two behaviours can be understood in a weak-coupling RG approach. If we allow spin-anisotropic Kondo interaction, and define dimensionless couplings $j_\perp = \rho_0 J_{K\perp}$ and $j_\parallel = \rho_0 J_{K\parallel}$, the perturbative RG flow for small couplings takes the form [88]

$$\beta(j_\perp) = j_\perp j_\parallel, \qquad \beta(j_\parallel) = j_\perp^2, \tag{35}$$

sketched in figure 6(*a*). There is a line of fixed points at $j_\perp = 0$, $j_\parallel \leqslant 0$, and initial couplings with $|J_\perp| \leqslant -J_\parallel$ flow towards this line, whereas for all other initial values the system flows to strong coupling. The line $|j_\perp| = -j_\parallel$ represents a line of transitions of the Kosterlitz–Thouless type. Such a transition also occurs in the classical $d = 2$ XY model (section 3.6.1); it turns out that the RG equations for the Kondo problem are exactly identical to the ones for the XY model. In particular, no critical fixed point exists, and power law critical behaviour is absent.

This well-established picture of the Kondo effect has to be revised for systems with vanishing conduction band DOS at the Fermi energy. This is the case in hard-gap systems where $\rho(\epsilon) = 0$ for energies smaller than the gap energy, $|\epsilon| < \Delta$ [89, 90], and in so-called pseudogap systems [91–94] with a power-law DOS $\rho(\epsilon) = \rho_0|\epsilon/D|^r$ ($r > 0$). The former situation is realized, e.g. in semiconductors and s-wave superconductors, whereas the latter arises in semimetals and in systems with long-range order where the order parameter has nodes at the Fermi surface, e.g. p- and d-wave superconductors ($r = 2$ and 1).

In systems with a hard gap in the conduction electron DOS, screening is impossible at small Kondo couplings, J_K, even at the lowest temperatures, which is easily understood by the absence of low-energy fermions (figure 5(*b*)). Interestingly, in the particle–hole symmetric case, screening does not occur even for large J_K, whereas in the absence of particle–hole symmetry an increase of the Kondo coupling eventually leads to a first-order boundary transition into a phase with Kondo screening—this transition is characterized by a simple level crossing between the doublet and singlet impurity states [89, 90].

The case of a power-law DOS is even more interesting: the pseudogap Kondo model shows a continuous boundary quantum phase transition at a critical Kondo coupling, J_c [91–93]. For small DOS exponents, r, the physics is captured by the RG equations

$$\beta(j_\perp) = -rj_\perp + j_\perp j_\parallel, \qquad \beta(j_\parallel) = -rj_\parallel + j_\perp^2 \tag{36}$$

(see figure 6(*b*)). There is now a critical fixed point at $j_\perp^* = j_\parallel^* = r$. Initial values located below the separatrix flow to the LM fixed point at $j = 0$, describing an unscreened impurity, whereas large j flow to SC. The resulting phase diagram is shown in figure 7(*a*). The behaviour at large r, as well as the SC physics, is not described by this RG; from comprehensive numerical studies [92,93] based on Wilson's NRG approach [22] it is known that the fixed-point structure changes for $r > \frac{1}{2}$, and furthermore particle–hole asymmetry is a relevant parameter in the SC regime for $r > 0$ (while being marginally irrelevant at $r = 0$).

For small r, critical properties of the pseudogap Kondo model can be calculated using the weak-coupling RG sketched before. This can be understood as an expansion about the lower-critical 'dimension' $r = 0$, similar to the expansion in $(2 + \epsilon)$ dimensions for the non-linear sigma model (18). Very recently, it has become clear that $r = 1$ plays the role of the upper-critical 'dimension' in the pseudogap Kondo problem. The universal critical theory in the vicinity of $r = 1$ can be formulated as a crossing of singlet and doublet impurity levels, coupled to low-energy conduction electrons—this is equivalent to an infinite-U single-impurity Anderson model with pseudogap DOS [94]. For $r < 1$ the coupling between

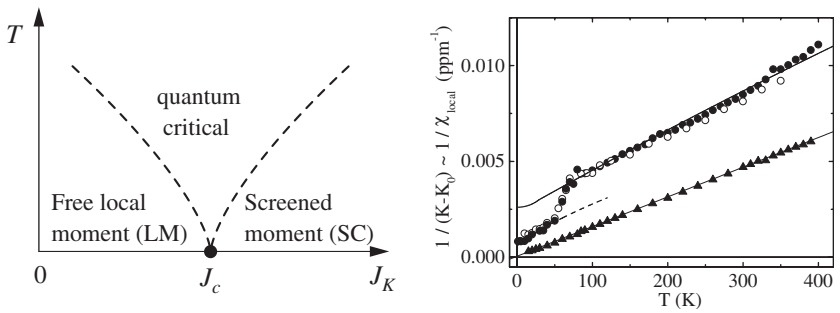

Figure 7. Left: phase diagram of the pseudogap Kondo model. At $T = 0$ the moment is screened at large J_K (SC), but unscreened at small J_K (LM). The two phases are separated by a continuous boundary transition at $J_K = J_c$; the quantum critical region is characterized by power laws, e.g. in the local susceptibility and the conduction electron T matrix [98, 99]. The crossover line between the quantum critical and the screened regimes can be loosely associated to the Kondo temperature. Right: temperature dependence of the inverse local susceptibility of dilute Li ions in $YBa_2Cu_3O_{6+x}$ (after [97]). The circles (▲) are data from optimally doped (underdoped) samples; the lines are Curie–Weiss fits. At optimal doping, the Weiss temperature changes significantly upon passing through the superconducting T_c, indicating that Kondo screening above T_c is stronger than below T_c. No change occurs in the underdoped sample, which should be attributed to the pseudogap above T_c. The data below T_c show a Weiss temperature $(-\Theta)$ of 40 K whereas $-\Theta$ is close to zero in the underdoped case—this suppression of Kondo screening likely corresponds to a boundary quantum phase transition.

impurity and conduction band is relevant under RG transformations, and the model allows an RG approach together with an expansion in $(1-r)$, in analogy to the expansion in $(4-\epsilon)$ dimensions of the ϕ^4 model (17). Critical exponents can be calculated in a $(1-r)$ expansion, and hyperscaling is obeyed. Conversely, for $r > 1$ perturbation theory is sufficient, and the transition can be characterized as level crossing with perturbative corrections, where hyperscaling is violated [94]. We note that slave–boson mean-field theory [91] reproduces a transition, but does not yield sensible critical behaviour. Alternatively, a dynamic multi-channel large-N approach [95] can be applied to the pseudogap Kondo problem, allowing a complete analytic low-energy solution both in the stable phases and at the QCPs, with non-trivial critical behaviour [96].

Experimentally, signatures of non-trivial Kondo physics have been observed in impurity-doped cuprate superconductors. Nominally non-magnetic Zn impurities (replacing Cu) have been shown to induce quasifree magnetic moments in their vicinity. The NMR data of [97] allowed one to fit the local impurity susceptibility to a Curie–Weiss law, where the Weiss temperature $(-\Theta)$ can be roughly identified with the Kondo temperature. This experiment indicates a strongly doping-dependent Kondo temperature, with T_K in the superconducting state ranging from 40 K around optimal doping to practically zero for strongly underdoped samples (see figure 7(*b*)). This qualitative change in the Kondo screening properties is a good candidate for a realization of the boundary quantum phase transition in the pseudogap Kondo model—there is no fundamental reason for this transition to coincide with any of the possible bulk phase transitions in the cuprates. As demonstrated in microscopic calculations [98,99], the boundary transition from screened to unscreened dilute impurity moments in superconducting cuprates is likely driven by the increase of the superconducting gap upon underdoping and/or by increasing antiferromagnetic host spin fluctuations that suppress fermionic Kondo screening (section 4.3). Kondo screening of the Zn moments around optimal doping also leads to a characteristic low-energy peak in the tunnelling signal as measured by STM (for further discussions see [98,100]).

Kondo physics in a superconducting environment can be observed in quantum dot systems too. A recent experiment [101] using a carbon nanotube dot coupled to Al leads shows a sharp crossover in the transport properties as a function of T_K/Δ, where T_K is the normal-state Kondo temperature of the dot and Δ the gap of the superconductor, consistent with the expectations within a hard-gap Kondo model.

4.2. Spin–boson and Bose–Kondo models

Systems of quantum impurities coupled to bosonic baths are an equally interesting model class; they have been first introduced in the context of the description of dissipative dynamics in quantum systems [102]. The simplest realization is the so-called spin–boson model, describing a spin or two-level system coupled to a single bath of harmonic oscillators. The Hamiltonian

$$H = -\frac{\Delta}{2}\sigma_x + \sum_{i\alpha}\omega_i a^\dagger_{i\alpha}a_{i\alpha} + \sum_{i\alpha}\frac{\sigma_\alpha}{2}\lambda_i(a_{i\alpha} + a^\dagger_{i\alpha}) \tag{37}$$

is a straightforward generalization of the spin–boson model to multiple baths: the a_α are vector bosons and can be interpreted as spin-1 excitations of a 'magnetic' bath. The couplings between spin and bosonic baths are completely specified by the bath spectral functions

$$J_\alpha(\omega) = \pi\sum_i \lambda^2_{i\alpha}\delta(\omega-\omega_i). \tag{38}$$

Of particular interest are power-law spectra

$$J_\alpha(\omega) = 2\pi\gamma_\alpha\omega_c^{1-s}\omega^s, \qquad 0<\omega<\omega_c, \quad s>-1, \tag{39}$$

where ω_c is a cutoff, and the dimensionless parameters γ_α characterize the coupling or dissipation strength.

In the conventional spin–boson model only $\gamma_z \neq 0$ ($\gamma_x = \gamma_y = 0$); then equation (37) describes a spin, tunnelling between $|\uparrow\rangle$ and $|\downarrow\rangle$ via Δ, and being damped by the coupling to the oscillator bath. The particular case of $s = 1$ corresponds to the well-studied Ohmic spin–boson model [102], which shows a Kosterlitz–Thouless quantum transition, separating a localized phase at $\gamma \geqslant \gamma_c$ from a delocalized phase at $\gamma < \gamma_c$ [102]. In the localized regime, the tunnel splitting between the two levels renormalizes to zero, i.e. the system gets trapped in one of the states $|\uparrow\rangle$ or $|\downarrow\rangle$, whereas the tunnel splitting stays finite in the delocalized phase. In the limit $\Delta \ll \omega_c$ the transition occurs at $\gamma_c = 1$.

Renewed interest in spin–boson models arises in the field of quantum computation, for modelling the coupling of qubits to a noisy environment; here also the case of a sub-Ohmic bath appears physically relevant. It has recently been established, using both perturbative RG for small $(1-s)$ and NRG, that the sub-Ohmic spin–boson model shows a continuous quantum transition between a localized and a delocalized phase for all bath exponents $0 < s < 1$ [103]. For fixed s there exists a single critical RG fixed point with s-dependent exponents; upon variation of s these fixed points form a line that terminates in the Kosterlitz–Thouless transition point at $s = 1$. Interestingly, this behaviour is somewhat similar to that of the particle–hole symmetric pseudogap Kondo model [92] described in section 4.1; however, for $s < 1$ and $r > 0$ the transitions in the two models are in different universality classes.

Models of the form (37) with a vector bath describe impurity moments embedded into quantum magnets, and are sometimes called Bose–Kondo models. The bosonic baths represent the host spin excitations: in a quantum paramagnet their spectrum is gapped, with the gap approaching zero at a zero-temperature magnetic ordering transition. (In dimensions $d < 3$ the bath Hamiltonian has to be supplemented by bosonic self-interactions, as these are strongly relevant, see section 2.7.) At a bulk QCP of an antiferromagnet in $d = 2+s$ space dimensions the bath spectra are given by equation (39). For $1 < d < 3$ the impurity model has remarkable properties [104]: the coupling between spin and bath is relevant in the RG sense and flows to an infrared-stable intermediate-coupling fixed point. The impurity spin is then characterized by power-law autocorrelations and various universal properties, e.g. a Curie response of a fractional effective spin. For a finite impurity concentration, this universal interaction between impurity moments and host spin fluctuations leads to universal impurity-induced damping of spin fluctuations in cuprate superconductors [104]—note that at the relevant spin fluctuation energies (e.g. 40 meV in $YBa_2Cu_3O_7$) possible Kondo screening of the moments can be safely ignored, as experimentally T_K is 40 K or lower [97].

4.3. Kondo effect and spin fluctuations

In particular in the context of strongly correlated electron systems, which often feature Fermi-liquid quasiparticles and strong spin fluctuations at the same time, the question of the interplay between fermionic and bosonic 'Kondo' physics arises. This naturally leads to so-called Fermi–Bose Kondo models where an impurity spin is coupled to both a fermionic and a bosonic bath. The RG analysis shows that the two bath couplings compete, i.e. fermionic Kondo screening is suppressed by strong host spin fluctuations [37, 99].

Recently, it has been proposed [99] that this interplay actually plays a role in high-T_c cuprates, where NMR experiments indicate that dilute impurity moments are screened at optimal doping, but T_K is essentially suppressed to zero in underdoped compounds [97] (see section 4.1). A Fermi–Bose Kondo model, taking into account both the pseudogap DOS of the Bogoliubov quasiparticles and the strong antiferromagnetic fluctuations, provides a natural

explanation: spin fluctuations increase with underdoping, thus strongly reducing T_K due to the vicinity to the boundary transition which exists even in the absence of a bosonic bath [99].

Interestingly, similar quantum impurity models also appear in variants of DMFTs for lattice systems [39]. Motivated by neutron scattering experiments [35] on the heavy-fermion compound $CeCu_{6-x}Au_x$ (see also section 3.2.3), which indicate momentum-independent critical dynamics at an antiferromagnetic ordering transition, a self-consistent version of the Fermi–Bose Kondo model has been proposed to describe such critical behaviour within an extended dynamical mean-field approach (EDMFT) [37]. In this scenario, the critical point of the lattice model is mapped onto a particular critical point of the impurity model.

4.4. Multi-channel and multi-impurity models

Kondo screening is strongly modified if two or more fermionic screening channels compete. Nozières and Blandin [105] proposed a two-channel generalization of the Kondo model, which shows overscreening associated with an intermediate-coupling fixed point and non-Fermi liquid behaviour in various thermodynamic and transport properties. In general, such behaviour occurs for any number of channels $K > 1$ coupled to a spin $\frac{1}{2}$, and does not require fine tuning of the Kondo coupling. However, it is unstable w.r.t. a channel asymmetry; thus a two-channel fixed point can be understood as a critical point between two (equivalent) stable single-channel fixed points.

Many of the low-energy properties of the two-channel and related Kondo models have been studied using conformal field theory techniques [95, 106]. Interestingly, the multi-channel Kondo fixed point is perturbatively accessible in the limit of large channel number ($K \gg 1$) [95, 105]. Experimental realizations have been discussed in the context of rare-earth compounds [107]; furthermore, proposals based on quantum dot devices have been put forward.

Models of two or more impurities offer a new ingredient, namely the exchange interaction, I, between the different impurity spins; it can arise both from direct exchange and from the Ruderman–Kittel–Kasuya–Yosida (RKKY) interaction mediated by the conduction electrons. This interimpurity interaction competes with Kondo screening of the individual impurities; in Kondo lattice models it can lead to a magnetic ordering transition. The simplest model of two spin-$\frac{1}{2}$ impurities has been thoroughly studied: here, a ground state singlet can be realized either by individual Kondo screening (if $I < T_K$) or by formation of an interimpurity singlet (if $I > T_K$). It has been shown that these two parameter regimes are continuously connected (without any phase transition) as I is varied in the generic situation without particle–hole symmetry. Notably, in the particle–hole symmetric case one finds a transition associated with an unstable non-Fermi-liquid fixed point [108, 109].

Quantum phase transitions generically occur in impurity models showing phases with different ground state spin. For two spin-$\frac{1}{2}$ impurities, this can be realized by coupling to a single conduction band channel only. In this case, a Kosterlitz–Thouless-type transition between a singlet and a doublet state occurs, associated with a secondary exponentially small energy scale in the Kondo regime [110]. The physics becomes even richer if multi-channel physics is combined with multi-impurity physics—here, a variety of fixed points including such with local non-Fermi liquid behaviour can be realized.

Experimentally, quantum dots provide an ideal laboratory to study systems of two or more 'impurities'—note that the local impurity states can arise either from spin or from charge degrees of freedom on each quantum dot. In particular, a number of experiments have been performed on coupled quantum dot systems that can be directly mapped onto models of two Kondo or Anderson impurities, and some indications for phase transitions have been

found [111]. In addition, experimental realizations of two-impurity models using magnetic adatoms on metallic surfaces appear possible.

5. Conclusions and outlook

This review has discussed aspects of zero-temperature phase transitions in quantum systems. The introductory sections have highlighted the general properties of these quantum transitions, pointing out similarities and differences between classical thermal and quantum phase transitions. Subsequently, we have described a number of specific bulk quantum phase transitions in condensed matter systems, emphasizing the important role of low-energy fermionic excitations in determining the critical behaviour. In particular, we have touched upon spin and charge ordering transitions, secondary pairing transitions in superconductors, as well as metal–insulator and superconductor–insulator transitions, and made contact with recent experiments in correlated electronic systems. Finally, we have discussed quantum transitions in impurity systems. These transitions are a particular realization of boundary quantum phase transitions, where only a part of the system becomes critical.

Let us recapitulate a few important aspects. The theoretical description of a particular phase transition usually starts out with the identification of the relevant variables, the most important one being the order parameter. Analytical studies then often proceed following the Landau–Ginzburg–Wilson approach: all degrees of freedom other than the order parameter fluctuations are integrated out, resulting in an effective theory in terms of the order parameter only; such a theory can often also be guessed using general symmetry arguments. However, in itinerant electron systems the existence of gapless particle–hole continua potentially leads to singularities in the order parameter theory, rendering it non-local. A more promising but technically difficult approach consists of not integrating out all degrees of freedom other than the order parameter, i.e. treating all soft modes in the system on the same footing. This has been followed for the ferromagnetic transition of both clean and dirty Fermi liquids [24], and in the somewhat simpler situation of secondary pairing transitions in d-wave superconductors [41]. A second caveat of analytical approaches is that they have to employ perturbative methods in analysing the field theories; those methods can fail in strongly coupled or strongly disordered systems. Alternatively, high-accuracy numerical simulations either of simple microscopic models or of order parameter field theories can be used to access quantum critical behaviour.

Conceptually, quantum phase transitions open a field of fascinating physics, being connected with the peculiar properties of the quantum critical ground state. The absence of quasiparticle excitations can lead to a variety of unsual finite-temperature phenomena in the quantum critical region, such as unconventional power laws and non-Fermi-liquid behaviour, that mask the properties of the stable phases. Recent years have seen an outburst of experimental activities studying quantum criticality in systems as diverse as high-temperature superconductors, quantum Hall systems, heavy-fermion materials, quantum magnets, and atomic gases. For explaining the plethora of experimental findings, progress on the theory side is required, in particular in understanding dynamical and transport properties near quantum criticality, together with the influence of disorder.

Quantum criticality can provide new perspectives in the study of correlated systems, where intermediate-coupling phenomena are hardly accessible by standard weak- or strong-coupling perturbative approaches. A promising route starts by identifying QCPs between stable phases, and then uses these as vantage points for exploring the whole phase diagram by expanding in the deviation from criticality. It is clear that we have just scratched the surface of much exciting progress to come.

Acknowledgments

The author is indebted to S Sachdev for many fruitful collaborations and countless discussions which contributed enormously to the writing of this paper. It is a pleasure to thank R Bulla, C Buragohain, E Demler, L Fritz, M Garst, A Georges, S Kehrein, M Kirćan, A Polkovnikov, T Pruschke, A Rosch, T Senthil, Q Si, N-H Tong, T Vojta, D Vollhardt, P Wölfle, and Y Zhang for illuminating conversations and collaborations over the last years. This work was supported by the Deutsche Forschungsgemeinschaft through Vo794/1-1, SFB 484, and the Center for Functional Nanostructures Karlsruhe.

References

[1] Sondhi S L, Girvin S M, Carini J P and Shahar D 1997 *Rev. Mod. Phys.* **69** 315
[2] Belitz D and Kirkpatrick T R 2000 *Dynamics: Models and Kinetic Methods for Non-Equilibrium Many-Body Systems* ed J Karkheck (Dordrecht: Kluwer)
[3] Sachdev S 1999 *Quantum Phase Transitions* (Cambridge: Cambridge University Press)
[4] Laughlin R B 1998 *Adv. Phys.* **47** 943
[5] Bitko D, Rosenbaum T F and Aeppli G 1996 *Phys. Rev. Lett.* **77** 940
[6] Coleman P 1999 *Physica* B **259–261** 353
[7] von Löhneysen H 1996 *J. Phys. Condens. Matter* **8** 9689
[8] Dagotto E 1994 *Rev. Mod. Phys.* **66** 763
Maple M B 1998 *J. Magn. Magn. Mater.* **177** 18
Orenstein J and Millis A J 2000 *Science* **288** 468
[9] Sachdev S 2000 *Science* **288** 475
[10] Kravchenko S V, Mason W E, Bowker G E, Furneaux J E, Pudalov V M and D'Iorio M 1995 *Phys. Rev.* B **51** 7038
[11] Ma S-K 1976 *Modern Theory of Critical Phenomena* (Reading: Benjamin)
[12] Goldenfeld N 1992 *Lectures on Phase Transitions and the Renormalization Group* (Reading: Addison-Wesley)
[13] Mott N F 1990 *Metal–Insulator Transitions* (London: Taylor and Francis)
[14] Widom B 1965 *J. Chem. Phys.* **43** 3892
[15] Wilson K G 1971 *Phys. Rev.* B **4** 3174
Wilson K G 1971 *Phys. Rev.* B **4** 3184
[16] Chakravarty S, Halperin B I and Nelson D R 1988 *Phys. Rev. Lett.* **60** 1057
Chakravarty S, Halperin B I and Nelson D R 1989 *Phys. Rev.* B **39** 2344
[17] Zhu L, Garst M, Rosch A and Si Q 2003 *Phys. Rev. Lett.* **91** 066404
[18] Belitz D and Kirkpatrick T R 2003 *J. Low Temp. Phys.* **126** 1107
[19] Belitz D, Kirkpatrick T R and Vojta T 1997 *Phys. Rev.* B **55** 9452
Belitz D, Kirkpatrick T R and Vojta T 2002 *Phys. Rev.* B **65** 165112
[20] Brezin E and Zinn-Justin J 1976 *Phys. Rev.* B **14** 3110
[21] Belitz D and Kirkpatrick T R 1994 *Rev. Mod. Phys.* **66** 261
[22] Wilson K G 1975 *Rev. Mod. Phys.* **47** 773
[23] Rosch A 2001 *Phys. Rev.* B **64** 1744077
[24] Belitz D, Kirkpatrick T R, Mercaldo M T and Sessions S L 2001 *Phys. Rev.* B **63** 174427
Kirkpatrick T R and Belitz D 2003 *Phys. Rev.* B **67** 024419
[25] Sachdev S 2003 *Rev. Mod. Phys.* **75** 913
[26] Ivanov D A, Lee P A and Wen X G 2000 *Phys. Rev. Lett.* **84** 3958
Chakravarty S, Laughlin R B, Morr D K and Nayak C 2001 *Phys. Rev.* B **63** 094503
[27] Hertz J A 1976 *Phys. Rev.* B **14** 1165
[28] Millis A J 1993 *Phys. Rev.* B **48** 7183
[29] Abanov Ar and Chubukov A V 2000 *Phys. Rev. Lett.* **84** 5608
Abanov Ar, Chubukov A V and Schmalian J 2003 *Adv. Phys.* **52** 119
[30] Tranquada J M, Axe J D, Ichikawa N, Nakamura Y, Uchida S and Nachumi B 1996 *Phys. Rev.* B **54** 7489
Tranquada J M 1998 *J. Phys. Chem. Solids* **59** 2150
[31] Emery V J, Kivelson S A and Tranquada J M 1999 *Proc. Natl. Acad. Sci. USA* **96** 8814
[32] Castellani C, Di Castro C and Grilli M 1995 *Phys. Rev. Lett.* **75** 4650

Castellani C, Di Castro C and Grilli M 1998 *J. Phys. Chem. Solids* **59** 1694
Caprara S, Sulpizi M, Bianconi A, Di Castro C and Grilli M 1999 *Phys. Rev.* B **59** 14980
[33] Zaanen J 1999 *Physica* C **317** 217
[34] Varma C M 1999 *Phys. Rev. Lett.* **83** 3538
[35] Schröder A, Aeppli G, Coldea R, Adams M, Stockert O, von Löhneysen H, Bucher E, Ramazashvili R and Coleman P 2000 *Nature* **407** 351
[36] Coleman P, Pépin C, Si Q and Ramazashvili R 2001 *J. Phys.: Condens. Matter* **13** 723
[37] Si Q, Rabello S, Ingersent K and Smith J L 2001 *Nature* **413** 804
Si Q, Rabello S, Ingersent K and Smith J L 2003 *Phys. Rev.* B **68** 115103
[38] Senthil T, Sachdev S and Vojta M 2003 *Phys. Rev. Lett.* **90** 216403
Senthil T, Vojta M and Sachdev S 2003 *Preprint* cond-mat/0305193
[39] Metzner W and Vollhardt D 1989 *Phys. Rev. Lett.* **62** 324
Georges A, Kotliar G, Krauth W and Rozenberg M J 1996 *Rev. Mod. Phys.* **68** 13
[40] Balents L, Fisher M P A and Nayak C 1998 *Int. J. Mod. Phys.* B **12** 1033
[41] Vojta M, Zhang Y and Sachdev S 2000 *Phys. Rev.* B **62** 6721
Vojta M, Zhang Y and Sachdev S 2000 *Phys. Rev. Lett.* **85** 4940
Vojta M, Zhang Y and Sachdev S 2000 *Int. J. Mod. Phys.* B **14** 3719
[42] Harris A B 1974 *J. Phys. C: Solid State Phys.* **7** 1671
[43] Chayes J, Chayes L, Fisher D S and Spencer T 1986 *Phys. Rev. Lett.* **57** 2999
[44] Grinstein G 1985 *Fundamental Problems in Statistical Mechanics VI* ed E G D Cohen (New York: Elsevier) p 147
[45] Fisher D S 1986 *Phys. Rev. Lett.* **56** 416
[46] McCoy B M and Wu T T 1968 *Phys. Rev.* **176** 631
McCoy B M and Wu T T 1969 *Phys. Rev.* **188** 982
[47] Imry Y and Wortis M 1979 *Phys. Rev.* B **19** 3580
[48] Cardy J L 1998 *Preprint* cond-mat/9806355
[49] Fisher D S 1995 *Phys. Rev.* B **51** 6411
[50] Griffiths R B 1969 *Phys. Rev. Lett.* **23** 17
[51] Sandvik A W 2002 *Phys. Rev. Lett.* **89** 177201
Vajk O P and Greven M 2002 *Phys. Rev. Lett.* **89** 177202
[52] Vojta T 2003 *Phys. Rev. Lett.* **90** 107202
[53] Pich C, Young A P, Rieger H and Kawashima N 1998 *Phys. Rev. Lett.* **81** 5916
Motrunich O, Mau S-C, Huse D A and Fisher D S 2000 *Phys. Rev.* B **61** 1160
[54] Kirkpatrick T R and Belitz D 1996 *Phys. Rev. Lett.* **76** 2571
Narayanan R, Vojta T, Belitz D and Kirkpatrick T R 1999 *Phys. Rev. Lett.* **82** 5132
[55] Castro-Neto A H, Castilla G and Jones B A 1998 *Phys. Rev. Lett.* **81** 3531
Castro-Neto A H and Jones B A 2000 *Phys. Rev.* B **62** 14975
[56] Williams G V M, Tallon J L and Loram J W 1998 *Phys. Rev.* B **58** 15053
Panagopoulos C, Tallon J L, Rainford B D, Xiang T, Cooper J R and Scott C A 2002 *Phys. Rev.* B **66** 064501
[57] Anderson P W 1958 *Phys. Rev.* **109** 1492
[58] Kramer B and MacKinnon A 1993 *Rep. Prog. Phys.* **56** 1469
[59] Abrahams E, Anderson P W, Licciardello D C and Ramakrishnan T V 1979 *Phys. Rev. Lett.* **42** 637
[60] Wegner F 1979 *Z. Phys.* B **35** 207
Wegner F 1980 *Z. Phys.* B **36** 209
[61] Gebhard F 1997 *The Mott Metal–Insulator Transition* (Berlin: Springer)
[62] Bulla R 1999 *Phys. Rev. Lett.* **83** 136
Bulla R, Costi T A and Vollhardt D 2001 *Phys. Rev.* B **64** 045103
[63] Altshuler B L and Aronov A G 1985 *Electron–Electron Interactions in Disordered Systems* ed A L Efros and M Pollak (Amsterdam: North-Holland)
[64] Lee P A and Ramakrishnan T V 1985 *Rev. Mod. Phys.* **57** 287
[65] Finkelstein A M 1983 *Zh. Eksp. Teor. Fiz.* **84** 168
Finkelstein A M 1983 *Sov. Phys. JETP* **57** 97
[66] Waffenschmidt S, Pfleiderer C and Löhneysen H v 1999 *Phys. Rev. Lett.* **83** 3005
[67] Huckestein B 1995 *Rev. Mod. Phys.* **67** 357
[68] Greiner M, Mandel O, Esslinger T, Hänsch T W and Bloch I 2002 *Nature* **415** 39
[69] Fisher M P A, Grinstein G and Girvin S M 1990 *Phys. Rev. Lett.* **64** 587
Herbut I 2001 *Phys. Rev. Lett.* **87** 137004

[70] Fisher M P A, Weichman P B, Grinstein G and Fisher D S 1989 *Phys. Rev.* B **40** 546
Fisher M P A 1990 *Phys. Rev. Lett.* **65** 923
[71] Mason N and Kapitulnik A 2002 *Phys. Rev.* B **64** 060504
[72] Read N and Sachdev S 1991 *Phys. Rev. Lett.* **66** 1773
Wen X-G 1991 *Phys. Rev.* B **44** 2664
[73] Senthil T and Fisher M P A 2000 *Phys. Rev.* B **62** 7850
Senthil T and Fisher M P A 2001 *Phys. Rev.* B **63** 134521
[74] Motrunich O I and Senthil T 2002 *Phys. Rev. Lett.* **89** 277004
Wen X G 2002 *Preprint* cond-mat/0210040
[75] Fradkin E and Shenker S 1979 *Phys. Rev.* D **19** 3682
[76] Anderson P W 1973 *Mater. Res. Bull.* **8** 153
Anderson P W 1987 *Science* **235** 1196
[77] Moessner R and Sondhi S L 2001 *Phys. Rev. Lett.* **86** 1881
[78] Fulde P, Penc K and Shannon N 2002 *Ann. Phys. (Leizig)* **11** 892
[79] Zhang S-C 1997 *Science* **275** 1089
Zhang S-C, Hu J P, Arrigoni E, Hanke W and Auerbach A 1999 *Phys. Rev.* B **60** 13070
[80] Kivelson S A, Fradkin E and Emery V J 1998 *Nature* **393** 550
[81] Lake B *et al* 2002 *Nature* **415** 299
[82] Hoffman J E, Hudson E W, Lang K M, Madhavan V, Eisaki H, Uchida S and Davis J C 2002 *Science* **295** 466
[83] Kivelson S A, Fradkin E, Oganesyan V, Bindloss I P, Tranquada J M, Kapitulnik A and Howald C 2003 *Rev. Mod. Phys.* **75** 1201
[84] Demler E, Sachdev S and Zhang Y 2001 *Phys. Rev. Lett.* **87** 067202
[85] Polkovnikov A, Vojta M and Sachdev S 2002 *Phys. Rev.* B **65** 220509
[86] Vojta M 2002 *Phys. Rev.* B **66** 104505
[87] Binder K 1983 *Phase Transitions and Critical Phenomena* vol 8, ed C Domb and J L Lebowitz (London: Academic)
Cardy J L 1996 *Scaling and Renormalization in Statistical Physics* (Cambridge: Cambridge University Press)
[88] Hewson A C 1997 *The Kondo Problem to Heavy Fermions* (Cambridge: Cambridge University Press)
[89] Shiba H 1968 *Prog. Theor. Phys.* **40** 435
Müller-Hartmann E and Zittartz J 1970 *Z. Phys.* **234** 58
Satori K, Shiba H, Sakai O and Shimizu Y 1992 *Phys. Soc. Japan* **61** 3239
[90] Chen K and Jayaprakash C 1998 *Phys. Rev.* B **57** 5225
[91] Withoff D and Fradkin E 1990 *Phys. Rev. Lett.* **64** 1835
[92] Bulla R, Pruschke T and Hewson A C 1997 *J. Phys.: Condens. Matter* **9** 10463
Bulla R, Glossop M T, Logan D E and Pruschke T 2000 *J. Phys.: Condens. Matter* **12** 4899
[93] Gonzalez-Buxton C and Ingersent K 1998 *Phys. Rev.* B **57** 14254
Ingersent K and Si Q 2002 *Phys. Rev. Lett.* **89** 076403
[94] Vojta M and Fritz L 2003 *Preprint* cond-mat/0309262
[95] Parcollet O, Georges A, Kotliar G and Sengupta A 1998 *Phys. Rev.* B **58** 3794
[96] Vojta M 2001 *Phys. Rev. Lett.* **87** 097202
[97] Bobroff J, Alloul H, MacFarlane W A, Mendels P, Blanchard N, Collin G and Marucco J-F 2001 *Phys. Rev. Lett.* **86** 4116
[98] Vojta M and Bulla R 2002 *Phys. Rev.* B **65** 014511
[99] Vojta M and Kirćan M 2003 *Phys. Rev. Lett.* **90** 157203
[100] Polkovnikov A, Sachdev S and Vojta M 2001 *Phys. Rev. Lett.* **86** 296
[101] Buitelaar M R, Nussbaumer T and Schönenberger C 2002 *Phys. Rev. Lett.* **89** 256801
[102] Leggett A J, Chakravarty S, Dorsey A T, Fisher M P A, Garg A and Zwerger W 1987 *Rev. Mod. Phys.* **59** 1
[103] Bulla R, Tong N-H and Vojta M 2003 *Phys. Rev. Lett.* **91** 170601
[104] Sachdev S, Buragohain C and Vojta M 1999 *Science* **286** 2479
Vojta M, Buragohain C and Sachdev S 2000 *Phys. Rev.* B **61** 15152
[105] Nozières P and Blandin A 1980 *J. Phys.* **41** 193
[106] Affleck I and Ludwig A W W 1991 *Nucl. Phys.* B **352** 849
Affleck I and Ludwig A W W 1991 *Nucl. Phys.* B **360** 641
Affleck I and Ludwig A W W 1993 *Phys. Rev.* B **48** 7297
[107] Cox D L and Zawadowski A 1998 *Adv. Phys.* **47** 599
[108] Jones B A and Varma C M 1987 *Phys. Rev. Lett.* **58** 843
Jones B A, Varma C M and Wilkins J W 1988 *Phys. Rev. Lett.* **61** 125

[109] Affleck I, Ludwig A W W and Jones B A 1995 *Phys. Rev.* B **52** 9528
[110] Vojta M, Bulla R and Hofstetter W 2002 *Phys. Rev.* B **65** 140405(R)
Hofstetter W and Schoeller H 2002 *Phys. Rev. Lett.* **88** 016803
[111] Van der Wiel W G, De Franceschi S, Elzerman J M, Tarucha S, Kouwenhoven L P, Motohisa J, Nakajima F and Fukui T 2002 *Phys. Rev. Lett.* **88** 126803
Kogan A, Granger G, Kastner M A, Goldhaber-Gordon D and Shtrikman H 2003 *Phys. Rev.* B **67** 113309